

1 Drivers of the tropospheric ozone budget throughout the 2 21st century under the medium-high climate scenario RCP 3 6.0

4
5 L. E. Revell^{1,2}, F. Tummon¹, A. Stenke¹, T. Sukhodolov^{1,3}, A. Coulon¹, E.
6 Rozanov^{1,3}, H. Garny⁴, V. Grewe⁴, and T. Peter¹

7 [1]{Institute for Atmospheric and Climate Science, ETH Zurich, Zurich, Switzerland}

8 [2]{Bodeker Scientific, New Zealand}

9 [3]{Physical-Meteorological Observatory/World Radiation Center, Davos, Switzerland}

10 [4]{DLR, Institut für Physik der Atmosphäre, Oberpfaffenhofen, Germany}

11 Correspondence to: L. E. Revell (laura.revell@env.ethz.ch)

12 13 **Abstract**

14 Because tropospheric ozone is both a greenhouse gas and harmful air pollutant, it is important
15 to understand how anthropogenic activities may influence its abundance and distribution
16 through the 21st century. Here, we present model simulations performed with the chemistry-
17 climate model SOCOL, in which spatially disaggregated chemistry and transport tracers have
18 been implemented in order to better understand the distribution and projected changes in
19 tropospheric ozone. We examine the influences of ozone precursor emissions (nitrogen oxides
20 (NO_x), carbon monoxide (CO) and volatile organic compounds (VOCs)), climate change
21 (including methane effects) and stratospheric ozone recovery on the tropospheric ozone
22 budget, in a simulation following the climate scenario Representative Concentration Pathway
23 (RCP) 6.0 (a medium-high, and reasonably realistic climate scenario). Changes in ozone
24 precursor emissions have the largest effect, leading to a global-mean increase in tropospheric
25 ozone which maximises in the early 21st century at 23% compared to 1960. The increase is
26 most pronounced at northern midlatitudes, due to regional emission patterns: between 1990
27 and 2060, northern midlatitude tropospheric ozone remains at constantly large abundances:
28 31% larger than in 1960. Over this 70 year period, attempts to reduce emissions in Europe and

1 North America do not have an effect on zonally-averaged northern midlatitude ozone because
2 of increasing emissions from Asia, together with the long lifetime of ozone in the troposphere.
3 A simulation with fixed anthropogenic ozone precursor emissions of NO_x, CO and non-
4 methane VOCs at 1960 conditions shows a 6% increase in global-mean tropospheric ozone by
5 the end of the 21st century, with an 11% increase at northern midlatitudes. This increase
6 maximises in the 2080s, and is mostly caused by methane, which maximises in the 2080s
7 following RCP 6.0, and plays an important role in controlling ozone directly, and indirectly
8 through its influence on other VOCs and CO. Enhanced flux of ozone from the stratosphere to
9 the troposphere as well as climate change-induced enhancements in lightning NO_x emissions
10 also increase the tropospheric ozone burden, although their impacts are relatively small.
11 Overall, the results show that under this climate scenario, ozone in the future is governed
12 largely by changes in methane and NO_x; methane induces an increase in tropospheric ozone
13 that is approximately one-third of that caused by NO_x. Climate impacts on ozone through
14 changes in tropospheric temperature, humidity and lightning NO_x remain secondary compared
15 with emission strategies relating to anthropogenic emissions of NO_x, such as fossil fuel
16 burning. Therefore, emission policies globally have a critical role to play in determining
17 tropospheric ozone evolution through the 21st century.

18

19 **1 Introduction**

20 Ozone is a key trace gas in the atmosphere, with approximately 90% residing in the
21 stratosphere and 10% in the troposphere. While stratospheric ozone is essential for shielding
22 life on Earth from harmful ultraviolet (UV-B) radiation, tropospheric ozone has harmful
23 effects because it is an air pollutant, with adverse effects on crop yields (and therefore food
24 security), visibility (affecting, for example, all forms of traffic) and human health (West et al.,
25 2007). Indeed, a recent study by Silva et al. (2013) found that anthropogenic ozone
26 contributes towards 470,000 respiratory deaths globally each year. Simultaneously,
27 tropospheric ozone is a greenhouse gas that has contributed significantly to climate change; it
28 has the third-highest pre-industrial to present day radiative forcing after carbon dioxide (CO₂)
29 and methane (CH₄) (Myhre et al., 2013; Stevenson et al., 2013). In addition to its roles in air
30 pollution and climate change, tropospheric ozone is important in determining the oxidation
31 capacity of the troposphere; the hydroxyl (OH) radical is principally produced from ozone,

1 and controls the lifetime of many atmospheric species such as CH₄, CO and NMVOCs (non-
2 methane volatile organic compounds), including some halocarbons (Thompson, 1992).

3

4 Ozone exists in the troposphere as a result of in situ chemical production and transport from
5 the stratosphere. Approximately 90% is produced via chemical reactions between nitrogen
6 oxides (NO_x = NO + NO₂), hydrocarbons and carbon monoxide (CO) during daylight hours
7 (Denman et al., 2007); therefore air pollution policy can be expected to play a significant role
8 in the evolution of tropospheric ozone through the 21st century and beyond. Depending on the
9 sensitivity of ozone budget reactions to humidity and temperature, the distribution and
10 abundance of tropospheric ozone may also be affected by climate change and changes in
11 transport and convection through the 21st century. Ozone can also be transported, either from
12 the stratosphere (stratosphere-troposphere exchange, abbreviated to STE), or within the
13 troposphere on long-range scales. Long-range ozone transport within the troposphere is
14 modulated by decadal climate variability (Lin et al., 2014). Transport of ozone from the
15 stratosphere is expected to increase through the 21st century as: (1) stratospheric ozone
16 abundances will increase, due to the phase-out of ozone-depleting halogenated substances
17 under the Montreal Protocol, and due to stratospheric cooling slowing the ozone destruction
18 cycles (Bekki et al., 2011); (2) stratosphere-to-troposphere transport of air will accelerate due
19 to a strengthening of the Brewer-Dobson circulation as projected by climate models, resulting
20 from enhanced tropospheric warming and convection, and subsequent wave activity (Butchart
21 et al., 2010; Kawase et al., 2011). Both effects will lead to enhanced down-welling of ozone
22 at mid- and polar latitudes. Stratospheric ozone recovery may further affect the evolution of
23 tropospheric ozone through decreased solar actinic flux to the troposphere, which slows
24 photolysis rates in the troposphere (Zhang et al., 2014).

25

26 In recent years as computational cost has declined, models which couple chemistry and
27 climate (chemistry-climate models, or CCMs) have become increasingly complex, with many
28 now including detailed tropospheric chemistry and other tropospheric processes. Morgenstern
29 et al. (2013) used the UM-UKCA CCM to look at how climate change, stratospheric ozone
30 recovery and methane affect ozone, although they did not consider future changes in non-
31 methane ozone precursors. They found that climate change and stratospheric ozone recovery
32 have approximately equal and opposite effects on surface ozone by 2050, resulting in an

1 increase in tropospheric ozone driven by methane. Doherty et al. (2013) also investigated
2 climate change-related effects on tropospheric ozone with an ensemble of three CCMs, and
3 found that increased temperature and water vapour influenced surface ozone more strongly
4 than climate change-induced enhancements in STE. Furthermore, several studies examining
5 tropospheric ozone budgets and changes over time from the ACCMIP (Atmospheric
6 Chemistry and Climate Model Intercomparison Project) ensemble of models have been
7 published recently (e.g. Bowman et al., (2013); Stevenson et al., (2013); Young et al. (2013)).
8 The ensemble mean of results obtained from ACCMIP provides a useful point of reference for
9 the results obtained in this study, and as such we refer to ACCMIP results later on.

10

11 To gain a clear insight into projected tropospheric ozone changes through the 21st century, we
12 have implemented a suite of chemistry and transport tracers into the SOCOL (Solar Climate
13 Ozone Links) CCM, and used them to disentangle the various factors influencing the ozone
14 budget in the free troposphere. Here we compare projected ozone changes in a future
15 reference simulation, which assumes emissions of NO_x, CO, CH₄ and NMVOCs according to
16 Representative Concentration Pathway (RCP) 6.0, with those in simulations with ozone
17 precursor emissions fixed at 1960 levels. Climate change and stratospheric ozone recovery
18 are fully simulated in both scenarios, and the chemistry and transport tracers allow us to
19 analyse their effects, for example by quantifying STE fluxes and tracking reaction rates for
20 key ozone budget reactions.

21

22 **2 Computational methods**

23 **2.1 The SOCOL chemistry-climate model**

24 In order to understand the influences of ozone precursor emissions and climate change on the
25 free tropospheric ozone budget (we focus mostly on the 500 hPa level), simulations were
26 performed with the SOCOL v.3 CCM. Its forerunner, SOCOL v.2, was extensively evaluated
27 in the SPARC CCMVal-2 activity (SPARC CCMVal, 2010) in two variants; SOCOL
28 operated by the ETH-Zurich group and NIWA-SOCOL operated by NIWA (National Institute
29 of Water and Atmospheric Research, New Zealand). Both compared reasonably with other
30 CCMs, obtaining performance grades in the midrange. Since then SOCOL has undergone
31 some significant improvements from version 2 to 3 (notably, the core general circulation

1 model has been updated, and the transport of chemical trace species is calculated with the
2 advection scheme of Lin and Rood (1996), rather than the hybrid scheme of Zubov et al.
3 (1999), which was used in SOCOL v.2). As a result, SOCOL v.3 shows more realistic
4 distributions of chemical trace species compared with its predecessors (both in the mean state
5 and also with respect to annual and interannual variability), and slower tropical upwelling in
6 the lower stratosphere; these changes, along with their effect on model performance, have
7 been documented in detail by Stenke et al. (2013).

8

9 SOCOL v.3 consists of the MEZON chemistry transport model (Egorova et al., 2003) and
10 MA-ECHAM5, the middle atmosphere version of the ECHAM general circulation model
11 (Roeckner et al., 2003), with 39 vertical levels between Earth's surface and 0.01 hPa (~80
12 km). For the present study, SOCOL was run with T42 horizontal resolution, which
13 corresponds approximately to $2.8^\circ \times 2.8^\circ$. Dynamical processes in SOCOL are calculated
14 every 15 minutes within the model, while radiative and chemical calculations are performed
15 every two hours.

16

17 Chemical constituents are advected by a flux-form semi-Lagrangian scheme (Lin and Rood,
18 1996), and the chemical solver algorithm uses a Newton-Raphson iterative method taking into
19 account 41 chemical species, 140 gas-phase reactions, 46 photolysis reactions, and 16
20 (stratospheric) heterogeneous reactions. Isoprene (C_5H_8) oxidation is accounted for with the
21 inclusion of the Mainz Isoprene Mechanism (MIM-1), which comprises 16 organic species
22 (degradation products of isoprene) and a further 44 chemical reactions (Poeschl et al., 2000).
23 Aside from isoprene and formaldehyde, we consider only the contribution to CO from other
24 NMVOCs; that is, a certain fraction of the NMVOC emission is directly added to CO. For
25 anthropogenic NMVOC emissions, the conversion factor to CO is 1.0, for biomass burning it
26 is 0.31, and for biogenic NMVOC emissions it is 0.83; these conversion factors were derived
27 from Ehhalt et al. (2001). Biogenic emissions are not interactive, but follow a climatology
28 (described in Section 2.2).

29

30 Photolysis rates are calculated at every chemical time step using a look-up-table approach
31 (Roazanov et al., 1999), including effects of the solar irradiance variability. The look-up tables

1 provide photolysis rates as a function of O₂ and O₃ columns, meaning that the photolysis
2 scheme sees interactive ozone. The impact of clouds on photolysis rates is accounted for by
3 including a cloud modification factor, following Chang et al. (1987). Interactive lightning
4 NO_x is calculated via a parameterization based on cloud top height (Price and Rind, 1992)
5 with local scaling factors calculated from the Lightning Imaging Sensor (LIS) and Optical
6 Transient Detector (OTD) satellite observations (Christian et al., 2003). Although the scaling
7 approach is widely used to improve the representation of the global distribution of lightning,
8 it carries some uncertainty as the future regions of lightning occurrence may differ from those
9 currently observed (Murray et al., 2012). Furthermore, the scaling approach may prevent
10 future changes in convective activity from modifying the magnitude of lightning NO_x
11 production.

12

13 The treatment of stratospheric aerosols in SOCOL is described by Stenke et al. (2013).
14 Tropospheric aerosols in SOCOL include sulfate, dust, sea salt, black carbon, organic carbon
15 and methane sulfonate. For the simulations presented here, we used a tropospheric aerosol
16 dataset, as described by Anet et al. (2013). Tropospheric aerosols are used to calculate local
17 heating rates and shortwave backscatter, however aerosol-cloud interactions and tropospheric
18 heterogeneous chemistry are not considered.

19

20 Key reaction rates for the ozone budget were saved in every model grid cell, enabling
21 chemistry to be analysed as a function of latitude, longitude, pressure and time. This approach
22 was successfully used by Revell et al. (2012) to study stratospheric ozone chemistry. To better
23 understand ozone transport, ozone tracers were implemented into SOCOL, based on the work
24 of Grewe (2006) and Garny et al. (2011). Following this approach, the global ozone mixing
25 ratio is disaggregated into 21 separate fields, according to in which of 21 predefined regions
26 (defined by latitude and pressure) of the atmosphere the ozone originated; this approach is
27 discussed further in Section 3.3.

28

29 To evaluate how realistically SOCOL simulates the distribution of tropospheric species, we
30 compared ozone, CO and NO₂ (three key components of the tropospheric ozone budget) with
31 satellite measurements over the period 2005-2009. Level 3 ozone and CO profile data were

1 taken from TES (Tropospheric Emission Spectrometer), a Fourier transform infrared
2 spectrometer onboard NASA's Aura satellite (e.g. Ho et al., 2009; Richards et al., 2008).
3 Tropospheric NO₂ columns were compared with those measured by OMI (Ozone Monitoring
4 Instrument) (Boersma et al., 2007).

5

6 **2.2 Emission scenarios**

7 SOCOL simulations were performed in support of the IGAC/SPARC Chemistry-Climate
8 Model Initiative (CCMI; Eyring et al., 2013a), and therefore the boundary conditions used
9 here adhere to the specifications of CCMI simulations, namely the REF-C2 and SEN-C2-
10 fEmis simulations (hereafter fEmis, for brevity). These transient simulations are described in
11 depth by Eyring et al. (2013a), but salient details are reproduced in Table 1. The REF-C2
12 simulation (1960-2100) was developed as a future reference simulation, to understand how
13 the atmosphere would evolve under “best guess” estimates of future greenhouse gas
14 concentrations, ozone-depleting substances (ODSs), ozone precursor emissions and sea-
15 surface temperatures (SSTs). REF-C2 is based on RCP 6.0, a medium-high climate change
16 scenario. Prescribed mixing ratios of greenhouse gases and long-lived chlorine, as well as
17 emission fluxes of surface NO_x, NMVOCs and CO for the REF-C2 simulation are shown in
18 Fig. 1. For biogenic isoprene, formaldehyde and other NMVOC emissions we use a
19 climatology for the year 2000 (based on a MEGAN (Model of Emissions of Gases and
20 Aerosols from Nature; Guenther et al. (2006)) run), while the biomass burning emissions
21 follow those described by Lamarque et al. (2010) until 2000, and RCP 6.0 thereafter.
22 Similarly, anthropogenic emissions of formaldehyde and other anthropogenic NMVOCs
23 follow Lamarque et al. (2010) until 2000, then RCP 6.0.

24

25 The fEmis “fixed emissions” simulation (1960-2100) is identical to REF-C2, except that non-
26 methane ozone precursor emissions are held constant at 1960 levels. For the present study,
27 this simulation allowed us to explore the question of how global tropospheric ozone would
28 evolve if air pollution remained at continuously low (1960) levels throughout the 21st century.
29 Because methane is also an air pollutant but not fixed at 1960 levels in the fEmis simulation
30 (as we are interested in its climate impact), we ran a fCH₄ “fixed methane” simulation for
31 1960-2100. The fCH₄ simulation used identical boundary conditions to the fEmis simulation,

1 except methane concentrations were held constant at 1960 levels (thus impacting both
2 chemistry and radiation directly).

3

4 Simulations were started in 1950 to allow ten years for the model to reach a steady state; this
5 spin-up period was subsequently discarded and not used in our analyses.

6

7 **3 Results and discussion**

8 **3.1 Evaluation of model performance**

9 Model simulated ozone, CO and NO₂ fields from the SOCOL REF-C2 simulation were
10 compared to satellite observations over the period 2005-2009 (Fig. 2). Ozone and CO profiles
11 were taken from TES and NO₂ columns from OMI. The WMO-defined tropopause was used
12 to calculate SOCOL NO₂ columns. SOCOL data were not processed with satellite operators
13 (such as averaging kernels). While this results in a less meaningful comparison, it has been
14 shown that only minor differences result from the application of satellite operators (Huijnen et
15 al., 2010). We chose the period 2005-2009 over which to compare data as it is representative
16 of the present day and because of good data availability for this period. Relative to TES,
17 SOCOL has a large positive ozone bias at 500 hPa of up to 30 ppb in the Northern
18 Hemisphere and tropics, and a smaller negative bias (~5-10 ppb) in the Southern Hemisphere
19 (Figs. 2a-c). Surface ozone in SOCOL is biased on a similar order of magnitude in the
20 Northern Hemisphere compared with the mid-troposphere, with ozone over Europe, the US
21 and Asia up to 20 ppb higher in 2000 compared with the ACCMIP ensemble mean (Young et
22 al., 2013).

23

24 One possibility for the large Northern Hemisphere bias might be a too-weak removal of NO_x
25 from the troposphere, which is described by the HNO₃ washout process. In the model setup
26 for the present study, a constant removal value was applied to the HNO₃ gas phase at each
27 time step (2.5% of gas-phase HNO₃ was removed everywhere up to 160 hPa, independent of
28 clouds or rainfall). Because HNO₃ can lead to ozone production when it is photolysed to form
29 NO₂, recently obtained results suggest that a more realistic removal process for HNO₃ (based
30 on in-cloud and below-cloud precipitation, and aerosol interaction (Chang, 1984; Seinfeld and

1 Pandis, 2006)) indeed reduces SOCOL's overly large ozone burden in the Northern
2 Hemisphere. However, the effect is not systematic, and this is not pursued in the present
3 study.

4

5 We note also that SOCOL is not alone among the current generation of models in
6 overestimating northern midlatitude ozone. Small systematic high biases in the Northern
7 Hemisphere and low biases in the Southern Hemisphere were also observed in the ACCMIP
8 models (Bowman et al., 2013, Young et al., 2013). ACCMIP included a range of models,
9 from coupled CCMs with comprehensive tropospheric and stratospheric chemistry, to
10 chemistry transport models (CTMs) which do not calculate meteorology online, and CCMs
11 with very simple tropospheric chemistry (Lamarque et al., 2013). Because the models used
12 the same emissions (as each other, and as in the present study), it was concluded that "the
13 prevalence of this bias could suggest they [the emissions] are deficient in some way, in either
14 their amount or distribution, or both." (Young et al., 2013). It is not clear whether SOCOL's
15 high ozone bias is a source issue (that is, emissions), a sink issue (HNO₃ washout), or a
16 combination of the two, and this requires further investigation. However, similar to the
17 ACCMIP models, SOCOL correlates spatially very well with observations, despite biases in
18 absolute ozone values; ozone concentrations are elevated in the Northern Hemisphere and
19 over Africa compared with the Southern Hemisphere, and low ozone concentrations are seen
20 over the tropical Pacific Ocean (discussed further in Section 3.2).

21

22 SOCOL simulates higher CO over regions where biomass burning is prevalent, namely South
23 America, Africa and Indonesia, than observed by TES (Figs. 2d-f). Southern Hemisphere CO
24 in SOCOL is in good agreement with TES, however in the Northern Hemisphere, CO is
25 biased low by 20-40 ppb. The low Northern Hemisphere CO bias is linked with the high
26 ozone bias in the same region, as ozone is the primary source of the OH radical, which in turn
27 oxidises CO. Similar biases in CO were observed in the ACCMIP models; at 500 hPa, the
28 multi-model mean is biased high compared with satellite observations over South America,
29 Africa and Indonesia, and thought to be linked to biomass burning emissions (Naik et al.,
30 2013). Furthermore, as seen in SOCOL, the multi-model mean is in good agreement with
31 observations in the Southern Hemisphere. The OH abundance is also in agreement with the
32 multi-model mean of the ACCMIP models; in the year 2000, the global tropospheric airmass-

1 weighted OH concentration is 11.5×10^5 molecules cm^{-3} , compared with the multi-model
2 mean of 11.7 ± 1.0 molecules cm^{-3} in the ACCMIP models (Voulgarakis et al., 2013).

3

4 SOCOL reproduces the elevated tropospheric NO_2 columns observed by OMI over North
5 America, Europe and Asia, but overestimates their magnitude (Figs. 2g-i); this is linked in
6 part to HNO_3 washout from the troposphere (as described above), and also leads to the
7 general high ozone bias in SOCOL throughout the Northern Hemisphere, which is likely
8 related to emissions. We note that potential discrepancies in emissions are a major source of
9 uncertainty in our analyses. Indeed, Parrish et al. (2014) identify emissions as an issue in need
10 of attention, given that CCMs consistently overestimate tropospheric ozone mixing ratios, and
11 underestimate the magnitude of tropospheric ozone changes over the past 50-60 years.

12

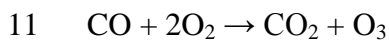
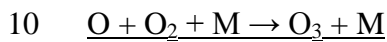
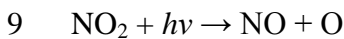
13 As discussed in Section 2.1, tropospheric aerosols are considered in SOCOL's radiation
14 scheme but not in the photolysis or heterogeneous chemistry schemes, which may be a further
15 reason for the tropospheric ozone biases. Dentener and Crutzen (1993) showed that N_2O_5
16 hydrolysis on tropospheric aerosols reduces the tropospheric ozone burden by 10-25%,
17 although the reaction probabilities they used were likely too large. Recent sensitivity
18 simulations with the SOCOL model show that tropospheric ozone is reduced by a maximum
19 of 10% when N_2O_5 hydrolysis is included in the model (following the parameterization of
20 Evans and Jacob (2005)), although some regions show a slight increase in tropospheric ozone.
21 Improving the treatment of tropospheric aerosols in SOCOL is the subject of ongoing
22 research, and is not further addressed here.

23

24 Although SOCOL is subject to several biases in terms of absolute species concentrations, it
25 captures the latitudinal and longitudinal distributions of ozone, CO and NO_2 convincingly.
26 Furthermore, given that the changes in ozone, NO_x , NMVOCs and CO over the period 2010-
27 2100 are on the same order magnitude as past changes between 1960-2010 (shown later in
28 Fig. 5), we do not expect non-linear feedbacks caused by the processes contributing to the
29 biases to severely compromise our results for the future. We now proceed to discuss the
30 distribution of ozone in the 1960s, and the model-simulated changes until 2100.

1 3.2 Tropospheric ozone chemistry

2 Although tropospheric ozone chemistry is comprehensive and complex, we outline below
3 some fundamental reaction cycles, as they are useful in discussing SOCOL's spatial ozone
4 distribution later in this section. In the troposphere, ozone is produced via reaction cycles that
5 begin with oxidation of a NMVOC or CO, as shown below:



12

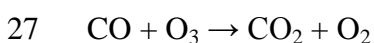
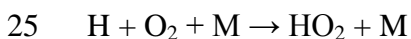
13 The reaction $\text{HO}_2 + \text{NO}$ is the rate-limiting step in ozone production and determines that the
14 net effect of this cycle is ozone production with a gross production rate R1. Other ozone
15 producing cycles follow the oxidation of VOCs, such as methane, formaldehyde, or isoprene
16 and its degradation products, leading to:



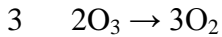
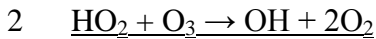
18 where R represents the organic chain of the molecules RO_2 and RO .

19

20 In contrast, when air is NO_x -poor, rather than reacting with NO , as in the ozone production
21 cycle R1 above, the generated peroxy radicals HO_2 (and generally RO_2), will instead react
22 with ozone, as in the cycles below, which are catalytic in HO_x , with ozone net loss rates R3
23 and R4:

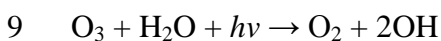
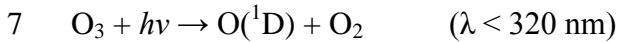


28



4

5 In the tropics, where humidity and solar actinic fluxes are high, the following reaction
6 mechanism R5 can become the leading ozone loss reaction, even though it is not catalytic:



10

11 In extremely NO_x -poor environments, ozone loss by R5 can occur to such a large extent that
12 minima in tropospheric ozone ensue, as in over the Amazon Basin and tropical Pacific Ocean
13 in Fig. 3a. Minima in tropical Western Pacific ozone have been observed in a number of
14 measurement campaigns (Kley et al., 1996; Singh et al., 1996; Tsutsumi et al., 2003; Rex et
15 al., 2014). Furthermore, Rex et al. (2014) showed, using ozone and OH measurements in
16 combination with the GEOS-Chem CTM, that very low tropospheric ozone and OH
17 abundances exist in the tropical Western Pacific. Rex et al. (2014) explained that low OH
18 abundances are concomitant with low ozone abundances in the tropical Western Pacific
19 because ozone is the principal source of OH, and ozone loss via R5 is so pronounced in this
20 region. They also noted that low NO_x abundances further reduce OH because production of
21 OH via $\text{HO}_2 + \text{NO} \rightarrow \text{OH} + \text{NO}_2$ becomes very slow (Gao et al., 2014). Results obtained from
22 SOCOL largely support this hypothesis, except that the OH and ozone minima are located in
23 slightly different places (over Indonesia and over the Western Pacific Ocean, respectively,
24 which was also found by Voulgarakis et al. (2013)). We suggest, therefore, that relatively
25 high abundances of CO and VOCs from biomass burning are important for OH depletion, in
26 combination with low NO_x abundances. The combination of high CO+VOCs and low NO_x
27 drives ozone loss via R3, and suppresses ozone production via R1. In addition, ozone loss by
28 R5 is fast because of high humidity and solar actinic fluxes in this region. Because ozone and
29 NO_x abundances are so low over Indonesia, the HO_x partitioning from HO_2 into OH (via

1 reaction of HO₂ with ozone in R3, and via reaction of HO₂ with NO in R1) becomes very
2 slow, resulting in low modelled OH abundances (Fig. 3b).

3

4 Figures 3c and d show the ratios of ozone production:loss, defined here as (R1 + R2)/(R3 +
5 R4 + R5) and NO_x:NMVOCs+CO, respectively. We consider CO and NMVOCs together as
6 they both undergo oxidation to initiate ozone production and destruction cycles. Here,
7 NMVOCs are C2-C5 species that are related to isoprene, belonging to the reduced mechanism
8 (MIM-1) outlined by Poeschl et al. (2000). One limitation of SOCOL is that the set of
9 NMVOCs included is very small, namely formaldehyde, isoprene and the 15 other isoprene
10 degradation products included in the MIM-1 isoprene oxidation mechanism. However, this
11 subset of NMVOCs makes the mechanism detailed enough to accurately reproduce the
12 diurnal cycle of important intermediate species like carbonyls, hydroperoxides and alkyl and
13 peroxy acyl nitrates, thus enabling the most relevant chemical processes for the tropospheric
14 ozone budget to be represented (Poeschl et al., 2000). As shown in Figs. 3c-d, regions with
15 high NO_x and low NMVOC+CO concentrations generally have high ozone production rates
16 relative to ozone loss.

17

18 **3.3 Projections for the 21st century**

19 Given the projected changes in ozone precursor emissions, greenhouse gases and stratospheric
20 ozone in the REF-C2 and fEmiss simulations, how is tropospheric ozone projected to evolve
21 through the 21st century? Further, are the projected changes dominated by changes in
22 precursor emissions or by changes in climate? We focus our tropospheric analysis in the mid-
23 troposphere, at 500 hPa. At this pressure the regional to hemispheric background ozone
24 concentration is established, and the signal is broadly consistent with the surface, as seen
25 when comparing Fig. 3a (ozone at 500 hPa) with Fig. 4 (surface ozone). Furthermore, most of
26 the tropospheric ozone transport between low, middle and high latitudes happens in the mid-
27 troposphere, as shown later in Fig. 7. 500 hPa is also high enough in the atmosphere to be
28 able to compare model output with satellite observations, as here the satellite instruments
29 have better sensitivity compared with closer to the surface (Fig. 2).

30

1 Figure 5 shows the model-simulated free tropospheric concentrations of NO_x and
2 NMVOCs+CO, as well as tropospheric and stratospheric ozone for the tropics and northern
3 and southern midlatitudes. For the stratosphere, Fig. 5d shows that extratropical stratospheric
4 column ozone is projected to increase through the 21st century in both the REF-C2 and fEmiss
5 simulations, owing to the phase-out of halocarbon gases under the Montreal Protocol on
6 Substances that Deplete the Ozone Layer. Because of CO_2 -induced cooling of the stratosphere
7 (Bekki et al., 2011) and the increased rate of tropical upwelling (Avallone and Prather, 1996),
8 the Northern and Southern Hemisphere stratospheric ozone columns increase to values
9 slightly higher than those in 1980 by the end of the 21st century. Projected accelerated tropical
10 upwelling is also expected to lead to slight decreases in tropical stratospheric ozone through
11 the 21st century, as seen here.

12

13 In the troposphere, the REF-C2 simulation shows that concentrations of NO_x , NMVOCs and
14 CO increase dramatically through the late 20th century (Figs. 5a-b), but eventually start to
15 decrease towards the end of the 21st century. Although anthropogenic NMVOC and CO
16 emissions are fixed at 1960 levels in the fEmiss simulation, an increase of CO still occurs as it
17 is an oxidation product of CH_4 , and CH_4 itself is not fixed at 1960 levels, but rather follows
18 RCP 6.0 (Masui et al., 2011).

19

20 Global-mean tropospheric ozone increases substantially through the 20th century in the REF-
21 C2 simulation, by 23% until the 2020s, stays at these high values for about 40 years, and then
22 decreases in the late 21st century (leading to an overall global-mean increase of 8% between
23 1960 and 2100). The global-mean tropospheric ozone burden decreases by 1% between 2000-
24 2030, and 10% between 2000-2100. These decreases are similar to the ensemble mean of the
25 ACCMIP models which performed the RCP 6.0 simulation, of 1% and 9% between 2000-
26 2030 and 2000-2100, respectively (Young et al., 2013).

27

28 One seemingly inconsistent feature of Fig. 5 is that at northern midlatitudes, NO_x and
29 NMVOC+CO concentrations decrease in the early 21st century, yet ozone concentrations in
30 the REF-C2 simulation remain constant. To explain this feature, one must examine the spatial
31 changes in ozone and its precursor emissions. Figures 6a-b show that NO_x and NMVOC+CO

1 both decrease in the Northern Hemisphere over Europe (and North America, in the case of
2 NO_x). Therefore, ozone decreases by up to 4% between the 2000s and 2020s over Europe
3 (Fig. 6c). However, the decrease in NO_x of approximately 20% over Europe and North
4 America is compensated for by up to a 40% increase in NO_x over Asia. In turn, this incurs an
5 increase in ozone of up to 6% in the same region, and, because of ozone's long lifetime in the
6 troposphere, the increase extends as far as the west coast of North America. The decreases in
7 ozone and its precursor emissions over Europe and North America and the increases over
8 Asia are statistically significant at the 95% level of confidence.

9

10 As shown in Fig. 6, changing regional emission patterns explain the substantial effect on
11 northern midlatitude tropospheric ozone (Fig. 5c): by 1990, tropospheric ozone is 31% higher
12 than in 1960, and such high abundances are sustained until 2060. Attempts by Europe and
13 North America to reduce emissions are offset by increases from Asia. It is well known that
14 ozone formed from precursor emissions in Asia can be transported across the Pacific Ocean to
15 the US, and this has previously been shown by, amongst others, Auvray et al. (2007),
16 Derwent et al. (2008) and Zhang et al. (2010). Europe may also expect to be affected by
17 increased emissions from other Northern Hemisphere sources in the early to mid-21st century;
18 Auvray and Bey (2005) showed that Asian and North American sources of ozone contribute
19 8% and 11% of the European annual ozone budget, respectively.

20

21 We further show decadal-mean ozone fluxes around the lower stratosphere and troposphere in
22 Fig. 7. 15 of the 21 tracer regions are shown, with the remaining six regions located in the
23 upper stratosphere above 30 hPa. Figure 7a quantifies ozone fluxes (Tg yr⁻¹) around the
24 boundary layer (850-1000 hPa) and free troposphere (100-850 hPa between 30°N-30°S and
25 200-850 hPa elsewhere), ascent of air from the tropics into the stratosphere, and downwelling
26 from the stratosphere at extratropical latitudes, for the 1960s. Figure 7b shows the same plot
27 for the 2050s, with increases of more than 20% since the 1960s marked in red; this serves to
28 highlight the increased export of ozone from tropical and northern midlatitude regions in the
29 troposphere and boundary layer to surrounding regions (such as northern high latitudes), due
30 to increased ozone production from precursor emissions in these regions between 1960-2050.

31

1 Decadal variability will also influence long-range transport of ozone within the troposphere
2 through the 21st century. Under RCP 6.0, there is an increased tendency towards more El Niño
3 conditions (consistent with the findings of e.g. Cai et al. (2014), although they examined RCP
4 8.5), which is linked with a strengthening of the flow of ozone-rich air from Europe and Asia
5 across the Pacific Ocean towards Hawaii in Northern Hemisphere autumn (Lin et al., 2014).
6 As El Niño conditions become increasingly prevalent, more eastward transport of ozone
7 across the Pacific Ocean may be expected to occur.

8

9 **3.4 Ozone change with fixed precursor emissions**

10 As shown in Figure 5b, holding CO and NMVOC emissions constant at 1960 levels does not
11 equate to constant concentrations of those species in the troposphere through the 21st century,
12 because methane is an important source of CO and an ozone precursor in its own right (e.g.,
13 Seinfeld and Pandis, 2006), and methane is not held constant in the fEmiss simulation. Figure
14 5c shows that in the absence of NO_x, the tropospheric ozone concentration maximises in the
15 2080s in the fEmiss simulation, which is approximately when methane concentrations
16 maximise following RCP 6.0 (Fig. 1a).

17

18 To understand the effect on tropospheric ozone abundances if all ozone precursors, including
19 methane, were held constant at 1960 levels, we ran an fEmiss simulation with fixed methane
20 (referred to as the fCH₄ simulation) for 1960-2100. Figure 5a shows that fixing methane does
21 not significantly impact NO_x concentrations. This demonstrates that modelled NO_x is driven
22 by chemistry, rather than climate-induced changes in meteorology. As noted in Section 2.1,
23 the scaling approach used to calculate lightning NO_x may not modify the magnitude of future
24 lightning NO_x production which might be expected to result from changes in convective
25 activity.

26

27 Figure 5b shows that compared with 1960, NMVOC+CO concentrations in the fCH₄
28 simulation are 5-10 ppb lower by the end of the 21st century at northern midlatitudes and in
29 the tropics, and decrease slightly at southern midlatitudes. In the 2080s, when methane
30 concentrations maximise following RCP 6.0, NMVOC+CO concentrations in the fCH₄

1 simulation are significantly lower than in the fEemis and REF-C2 simulations: in the global
2 average, NMVOC+CO concentrations are 4% lower in the fEemis simulation compared with
3 the REF-C2, and 22% lower in the fCH₄ simulation compared with the REF-C2. This
4 corroborates the finding of Wang and Prinn (1999), that controlling methane emissions is
5 more effective in controlling NMVOC+CO concentrations in the troposphere, than
6 controlling NMVOC+CO emissions themselves.

7

8 Figure 5c shows that tropospheric ozone concentrations in the 2080s of the fCH₄ simulation
9 are approximately the same as in the 1960s. In the global mean, ozone in the fCH₄ simulation
10 is 16% lower than in the REF-C2 simulation and 10% lower than in the fEemis simulation.
11 Methane has been shown to be an important ozone precursor historically, with both Shindell
12 et al. (2009) and Lang et al. (2012) finding it to be responsible for most of the tropospheric
13 ozone increase from pre-industrial to present times. Studies that have modelled projected
14 tropospheric ozone under the different RCPs find methane to be the largest factor defining
15 differences between the projections, because the RCPs assume huge reductions in NO_x and
16 NMVOCs, but project growth in methane, especially in RCP 8.5 (Wild et al., 2012; Eyring et
17 al. 2013b; Young et al., 2013).

18

19 **3.5 Impacts of climate change and stratospheric ozone recovery**

20 Although the fEemis simulation was designed to assess the impacts of climate change on the
21 atmosphere (Eyring et al., 2013a), there is a discrepancy with respect to methane's dual roles
22 as a greenhouse gas and ozone precursor when it comes to analyzing tropospheric ozone, as
23 discussed in the preceding section. However, given that ozone in the fCH₄ simulation is the
24 same in the 1960s and 2090s (Fig. 5c), this implies that the effects of climate change and
25 stratospheric ozone recovery on ozone in the mid-troposphere are either negligible, or offset
26 one another.

27

28 Climate change is thought to lead to tropospheric ozone decreases, due to increasing
29 temperature and humidity, which accelerates the ozone destruction reactions (e.g. Toumi et
30 al., 1996; Grewe et al., 2001; Doherty et al. 2013; Morgenstern et al., 2013). Figure 8a shows

1 the ozone change at 500 hPa in the fEemis simulation between the 1960s and 2090s. The
2 change is statistically significant at the 95% confidence level almost everywhere. Here, with
3 NO_x , NMVOCs and CO fixed in the fEemis simulation, ozone increases up to 6 ppb (a global-
4 mean increase of 6%). The only exceptions are south of 50°S, where it remains unchanged
5 and over the equatorial Pacific, where decreases of up to 2 ppb are seen. As discussed in
6 Section 3.2, the $\text{H}_2\text{O} + \text{O}(^1\text{D})$ reaction (R5) is very important for ozone loss over the remote
7 tropical Pacific Ocean, and this reaction becomes faster over the period 1960-2100 as the
8 troposphere becomes increasingly warm and humid (e.g. Zeng et al., 2010; Stevenson et al.,
9 2013). Figure 8b shows the change in the ozone production:loss ratio $(\text{R1}+\text{R2})/(\text{R3}+\text{R4}+\text{R5})$
10 between the 1960s and 2090s. This ratio decreases everywhere due to the increased rate of
11 ozone loss reactions, particularly at northern midlatitudes. Clearly temperature and humidity
12 play an important role for ozone in the tropical Pacific (leading to less ozone), however ozone
13 production resulting from the increase in methane is more important elsewhere, despite the
14 increased rate of the ozone destruction reactions.

15

16 Alongside methane, two further factors contribute to the ozone increase in the fEemis
17 simulation, although their influence is small: NO_x emissions from lightning, and STE. STE is
18 projected to increase through the 21st century, because (a) as lower stratospheric ozone
19 abundances increase, there is more ozone in the stratosphere available to be transported to the
20 troposphere, and (b) the overall meridional circulation, the Brewer-Dobson circulation, is
21 projected to strengthen (thus transporting more ozone from the stratosphere to the
22 troposphere) (Hegglin and Shepherd, 2009; Zeng et al., 2010). Figure 8c shows the
23 contribution of stratospheric ozone to the ozone budget at 500 hPa in the 1960s, calculated
24 using the lower-stratospheric ozone tracers. The tracers define the lower stratosphere as the
25 region between 30-200 hPa for 30-90°N and 30-90°S, and between 30-100 hPa for 30°N-30°S
26 (Fig. 7), given that the tropopause sits at a lower pressure level in the tropics. In the 1960s,
27 STE contributes between 0.1 – 5% of ozone present at 500 hPa. We calculate a total flux from
28 the lower stratosphere to the troposphere of 462 Tg yr^{-1} in the 1960s. This is lower than the
29 mean value from the model studies reviewed by Wild (2007) of 636 Tg yr^{-1} , but still within
30 one standard deviation from their mean. Figure 8d shows the change in the contribution of
31 stratospheric ozone to ozone at 500 hPa between the 1960s and 2090s in the fEemis simulation.

1 STE contributes up to one additional ppb at southern midlatitudes, and this is statistically
2 significant at the 95% confidence level.

3

4 As discussed in Section 3.2, methane leads to ozone production in the presence of NO_x . Along
5 with humidity and STE, lightning NO_x emissions may increase in a warmer climate, either
6 due to increased frequency of thunderclouds (and therefore lightning), or more intense
7 thunderstorms (Schumann and Huntrieser 2007; Price 2013). Figure 9a shows lightning NO_x
8 emissions from SOCOL averaged over the 1960s, and shows that most lightning is produced
9 over Africa and South America. Lightning NO_x emissions increase over the continents by
10 61% between 1960-2100 (Fig. 9b), and by 48% between 2000-2100. Smyshlyaev et al. (2010)
11 found that ozone increased between 10-20% when lightning NO_x emissions increased by 2
12 Tg(N) year^{-1} (depending on latitude and season), and up to 90% with a 20 Tg(N) year^{-1}
13 increase in lightning NO_x . Banerjee et al. (2014) calculated increases in lightning NO_x
14 emissions of 33% (2 Tg(N) year^{-1}) and 78% (4.7 Tg(N) year^{-1}) between 2000-2100 in
15 simulations using RCP 4.5 and RCP 8.5, respectively. In our fEemis simulation (which used
16 RCP 6.0, a scenario of intermediate severity compared to RCP 4.5 and RCP 8.5), we calculate
17 a 48% increase in lightning NO_x emissions over the same period, which is broadly consistent
18 with their findings. Banerjee et al. (2014) also showed that under RCP 8.5, the increase in
19 lightning NO_x emissions of 78% caused ozone increases of up to 30% in the troposphere
20 (maximizing between the equator and 30 °S). Although we cannot quantify ozone increases
21 induced by lightning NO_x emissions in our simulations, the studies referred to here indicate
22 the likely magnitude of increase (20-30%). Together with STE, ozone increases induced by
23 lightning NO_x emissions are largely offset by the temperature-induced increased rates of
24 ozone destruction in the troposphere. Finally, we note that the results also depend on the
25 chosen lightning parameterization, which is coupled to the cloud top heights; Grewe (2009)
26 showed that lightning NO_x emissions might also slightly decrease, when stronger but fewer
27 convective events occur in a future climate.

28

29 **4 Conclusions**

30 We have presented three CCM simulations covering the period 1960-2100, where the only
31 factors differing in the model setup were the ozone precursor emissions (NO_x , NMVOCs, CO
32 and CH_4). The tropospheric extension to the SOCOL CCM is still new and with 17 NMVOCs

1 only moderately sophisticated relative to some of the better-established tropospheric
2 chemistry models, however the results presented here compare favorably with previous work.

3

4 In the REF-C2 simulation, which used RCP 6.0 greenhouse gases and ozone precursors, the
5 maximum impact of ozone precursors on tropospheric ozone occurs between 1990 and 2060,
6 when global-mean ozone in the free troposphere increases by 23% from 1960 levels.
7 Although decreasing emissions of ozone precursor gases over Europe and North America lead
8 to local reductions in ozone in the early 21st century, large increases in precursor gas
9 emissions from Asia, combined with ozone's ability to be transported on inter-continental
10 scales within the troposphere, lead to a 70 year period between 1990-2060 in which ozone
11 abundances at northern midlatitudes are constantly elevated. In the late 21st century,
12 reductions in ozone precursor gases, especially NO_x, lead to decreases in tropospheric ozone
13 globally. However, global-mean concentrations are still 8% higher in the 2090s compared
14 with the 1960s.

15

16 In the fEmis (fixed ozone precursor emissions) simulation, global-mean ozone increases by
17 6% between 1960-2100, mostly because methane concentrations were not held constant. A
18 fCH₄ sensitivity simulation with all ozone precursors (including methane) held constant
19 shows that tropospheric ozone concentrations are the same in 2100 as in 1960. Increased flux
20 of ozone from the stratosphere to the troposphere, and increased emissions of NO_x from
21 lightning in a warmer climate contribute to increases in tropospheric ozone through the 21st
22 century, although their effects are largely offset by temperature-induced increased rates of
23 ozone destruction in the troposphere. Other climate-change related factors we have not
24 examined include biogenic emissions, which are thought to increase with temperature, but are
25 not considered in our simulations because SOCOL does not include an interactive scheme for
26 biogenic emissions. Notably, we have considered only a single climate change scenario (RCP
27 6.0), and the impacts of climate change will differ under different climate scenarios. We
28 furthermore reiterate that emissions of ozone precursor gases are also a significant source of
29 uncertainty in our results.

30

1 Overall, and given the assumptions inherent in the climate and ozone precursor emissions
2 scenarios we used, anthropogenic NO_x emissions have the largest influence on tropospheric
3 ozone in our simulations. Methane has the second largest influence, which is approximately
4 one-third that of anthropogenic NO_x emissions. We therefore conclude that emission policies
5 globally have the largest role to play in determining tropospheric ozone evolution through the
6 21st century.

7

8 **Acknowledgements**

9 LER is supported under the ETH Zurich Postdoctoral Fellowship Program. AC and AS are
10 supported by the Competence Center Environment and Sustainability (CCES) under the
11 project MAIOLICA-2. AS is furthermore supported by the SNSF under grant no.
12 200021_138037/1 (FuMES). FT is supported by a SNSF post-doctoral grant. We
13 acknowledge the free use of tropospheric NO₂ column data from the OMI sensor from
14 www.temis.nl. The authors would like to thank two anonymous reviewers for their helpful
15 comments on this manuscript.

16

1 **References**

- 2 Anet, J. G., Rozanov, E. V., Muthers, S., Peter, T., Brönnimann, S., Arfeuille, F., Beer, J.,
3 Shapiro, A. I., Raible, C. C., Steinhilber, F. and Schmutz, W. K.: Impact of a potential
4 21st century “grand solar minimum” on surface temperatures and stratospheric ozone,
5 *Geophys. Res. Lett.*, 40, 4420-4425, doi:10.1002/grl.50806, 2013.
- 6 Auvray, M. and Bey, I.: Long-range transport to Europe: Seasonal variations and implications
7 for the European ozone budget, *J. Geophys. Res.*, 110, D11303, doi:
8 10.1029/2004JD005503, 2005.
- 9 Auvray, M., Bey, I., Lllull, E., Schultz, M. G. and Rast, S.: A model investigation of
10 tropospheric ozone chemical tendencies in long-range transported pollution plumes, *J.*
11 *Geophys. Res.*, 112, D05304, doi:10.1029/2006JD007137, 2007.
- 12 Avallone, L. M. and Prather, M. J.: Photochemical evolution of ozone in the lower tropical
13 stratosphere, *J. Geophys. Res.*, 101(D1), 1457-1461, doi:10.1029/95JD03010, 1996.
- 14 Banerjee, A., Archibald, A. T., Maycock, A. C., Telford, P., Abraham, N. L., Yang, X.,
15 Braesicke, P. and Pyle, J. A.: Lightning NO_x, a key chemistry-climate interaction:
16 impacts of future climate change and consequences for tropospheric oxidizing
17 capacity, *Atmos. Chem. Phys.*, 14, 9871-9881, doi:10.5194/acp-14-9871-2014, 2014.
- 18 Bekki, S., Bodeker, G. E. (Coordinating Lead Authors), Bais, A. F., Butchart, N., Eyring, V.,
19 Fahey, D. W., Kinnison, D. E., Langematz, U., Mayer, B., Portmann, R.W., Rozanov,
20 E., Braesicke, P., Charlton-Perez, A. J., Chubarova, N. E., Cionni, I., Diaz, S. B.,
21 Gillett, N. P., Giorgetta, M. A., Komala, N., Lefèvre, F., McLandress, C., Perlwitz, J.,
22 Peter, T., and Shibata, K.: Future ozone and its impact on surface UV, Chapter 3 in:
23 *Scientific Assessment of Ozone Depletion: 2010, Global Ozone Research and*
24 *Monitoring Project – Report No. 52, 516 pp., World Meteorological Organization,*
25 *Geneva, Switzerland, 2011.*
- 26 Boersma, K. F., Eskes, H. J., Veefkind, J. P., Brinksma, E. J., van der A, R. J., Sneep, M.,
27 van den Oord, G. H. J., Levelt, P. F., Stammes, P., Gleason, J. F. and Bucsela, E. J.:
28 Near-real time retrieval of tropospheric NO₂ from OMI, *Atmos. Chem. Phys.*, 2103-
29 2128, doi:10.5194/acp-7-2103-2007, 2007.

- 1 Bowman, K. W., Shindell, D. T., Worden, H. M., Lamarque, J. F., Young, P. J., Stevenson, D.
2 S., Qu, Z., de la Torre, M., Bergmann, D., Cameron-Smith, P. J., Collins, W. J.,
3 Doherty, R., Dalsøren, S. B., Faluvegi, G., Folberth, G., Horowitz, L. W., Josse, B.
4 M., Lee, Y. H., MacKenzie, I. A., Myhre, G., Nagashima, T., Naik, V., Plummer, D.
5 A., Rumbold, S. T., Skeie, R. B., Strode, S. A., Sudo, K., Szopa, S., Voulgarakis, A.,
6 Zeng, G., Kulawik, S. S., Aghedo, A. M., and Worden, J. R.: Evaluation of ACCMIP
7 outgoing longwave radiation from tropospheric ozone using TES satellite
8 observations, *Atmos. Chem. Phys.*, 13, 4057-4072, doi:10.5194/acp-13-4057-2013,
9 2013.
- 10 Butchart, N., Cionni, I., Eyring, V., Shepherd, T. G., Waugh, D. W., Akiyoshi, H., Austin, J.,
11 Brühl, C., Chipperfield, M. P., Cordero, E., Dameris, M., Deckert, R., Dhomse, S.,
12 Frith, S. M., Garcia, R. R., Gettelman, A., Giorgetta, M. A., Kinnison, D. E., Li, F.,
13 Mancini, E., McLandress, C., Pawson, S., Pitari, G., Plummer, D. A., Rozanov, E.,
14 Sassi, F., Scinocca, J. F., Shibata, K., Steil, B., and Tian, W.: Chemistry-climate model
15 simulations of twenty-first century stratospheric climate and circulation changes, *J.*
16 *Climate*, 23, 5349-5374, doi:http://dx.doi.org/10.1175/2010JCLI3404.1, 2010.
- 17 Cai, W., Borlace, S., Lengaigne, M., van Rensch, P., Collins, M., Vecchi, G., Timmermann,
18 A., Santoso, A., McPhaden, M. J., Wu, L., England, M. H., Wang, G., Guilyardi, E.
19 and Jin, F.-F.: Increasing frequency of extreme El Niño events due to greenhouse
20 warming, *Nat. Clim. Change*, 4, 111-116, doi:10.1038/nclimate2100, 2014.
- 21 Chang, J. S., Brost, R. A., Isaksen, I. S. A., Madronich, S., Middleton, P., Stockwell, W. R.
22 and Walcek, C. J.: A three-dimensional Eulerian acid deposition model: Physical
23 concepts and formulation, *J. Geophys. Res.*, 92(D12), 14681-14700,
24 doi:10.1029/JD092iD12p14681, 1987.
- 25 Chang, T. Y.: Rain and snow scavenging of HNO₃ vapor in the atmosphere, *Atmos. Environ.*,
26 18(1), 191-197, doi:10.1016/0004-6981(84)90242-7, 1984.
- 27 Christian, H. J., Blakeslee, R. J., Boccippio, D. J., Boeck, W. L., Buechler, D. E., Driscoll, K.
28 T., Goodman, S. J., Hall, J. M., Koshak, W. J., Mach, D. M. and Stewart, M. F.:
29 Global frequency and distribution of lightning as observed from space by the Optical
30 Transient Detector, *J. Geophys. Res.*, 108(D1), doi:10.1029/2002JD002347, 2003.

- 1 Denman, K. L., Brasseur, G., Chidthaisong, A., Ciais, P., Cox, P. M., Dickinson, R. E.,
2 Hauglustaine, D., Heinze, C., Holland, E., Jacob, D., Lohmann, U., Ramachandran, S.,
3 da Silva Dias, P. L., Wofsy, S. C. and Zhang, X.: Couplings between changes in the
4 climate system and biogeochemistry, Chapter 7 in *Climate Change 2007: the Physical
5 Science Basis. Contribution of Working Group I to the Fourth Assessment Report of
6 the Intergovernmental Panel on Climate Change*, edited by S. Solomon, D. Qin, M.
7 Manning, Z. Chen, M. Marquis, K. B. Averyt, M. Tignor and H. L. Miller, Cambridge
8 University Press, Cambridge, United Kingdom and New York, NY, USA, 2007.
- 9 Dentener, F. J. and Crutzen, P. J.: Reaction of N_2O_5 on tropospheric aerosols: Impact on the
10 global distributions of NO_x , O_3 and OH, *J. Geophys. Res.*, 98(D4), 7149-7163,
11 doi:10.1029/92JD02979, 1993.
- 12 Derwent, R. G., Stevenson, D. S., Doherty, R. M., Collins, W. J. and Sanderson, M. G.: How
13 is surface ozone in Europe linked to Asian and North American NO_x emissions?
14 *Atmos. Environ.*, 42(32), 7412-7422, doi:10.1016/j.atmosenv.2008.06.037, 2008.
- 15 Doherty, R. M., Wild, O., Shindell, D. T., Zeng, G., MacKenzie, I. A., Collins, W. J., Fiore,
16 A. M., Stevenson, D. S., Dentener, F. J., Schultz, M. G., Hess, P., Derwent, R. G. and
17 Keating, T. J.: Impacts of climate change on surface ozone and intercontinental ozone
18 pollution: A multi-model study, *J. Geophys. Res.*, 118, 3744-3763,
19 doi:10.1002/jgrd.50266, 2013.
- 20 Egorova, T. A., Rozanov, E. V., Zubov, V. A. and Karol, I. L.: Model for investigating ozone
21 trends (MEZON), *Izv. Atmos. Ocean. Phys.*, 39, 277–292, 2003.
- 22 Ehhalt, D., Prather, M., Dentener, F., Derwent, R., Dlugokencky, E., Holland, E., Isaksen, I.,
23 Katima, J., Kirchhoff, V., Matson, P., Midgley, P. and Wang, M.: Atmospheric
24 chemistry and greenhouse gases, Chapter 4 in *Climate Change 2001: The Scientific
25 Basis. Contribution of Working Group I to the Third Assessment Report of the
26 Intergovernmental Panel on Climate Change*, edited by Houghton, J. T., Ding, Y.,
27 Griggs, D. J., Noguera, M., van der Linden, P. J., Dai, X., Maskell, K. and Johnson, C.
28 A, Cambridge University Press, Cambridge, United Kingdom and New York, NY,
29 USA, 2001.

- 1 Evans, M. J. and Jacob, D. J.: Impact of new laboratory studies of N₂O₅ hydrolysis on global
2 model budgets of tropospheric nitrogen oxides, ozone and OH, *Geophys. Res. Lett.*,
3 32, L09813, doi:10.1029/2005GL022469, 2005.
- 4 Eyring, V., Lamarque, J.-F., Hess, P., Arfeuille, F., Bowman, K., Chipperfield, M. P.,
5 Duncan, B., Fiore, A., Gettelman, A., Giorgetta, M. A., Granier, C., Hegglin, M.,
6 Kinnison, D., Kunze, M., Langematz, U., Luo, B., Martin, R., Matthes, K., Newman,
7 P. A., Peter, T., Robock, A., Ryerson, T., Saiz-Lopez, A., Salawitch, R., Schultz, M.,
8 Shepherd, T. G., Shindell, D., Staehelin, J., Tegtmeier, S., Thomason, L., Tilmes, S.,
9 Vernier, J.-P., Waugh, D. W. and Young, P. J.: Overview of IGAC/SPARC
10 Chemistry-Climate Model Initiative (CCMI) Community Simulations in Support of
11 Upcoming Ozone and Climate Assessments, *SPARC Newsletter* no. 40, ISSN 1245-
12 4680, 48-66, 2013a.
- 13 Eyring, V., Arblaster, J. M., Cionni, I., Sedláček, J., Perlwitz, J., Young, P. J., Bekki, S.,
14 Bergmann, D., Cameron-Smith, P., Collins, W. J., Faluvegi, G., Gottschaldt, K.-D.,
15 Horowitz, L. W., Kinnison, D. E., Lamarque, J.-F., Marsh, D. R., Saint-Martin, D.,
16 Shindell, D. T., Sudo, K., Szopa, S. and Watanabe, S.: Long-term ozone changes and
17 associated climate impacts in CMIP5 simulations, *J. Geophys. Res.*, 118, 5029-5060,
18 doi:10.1002/jgrd.50316, 2013b.
- 19 Gao, R. S., Rosenlof, K. H., Fahey, D. W., Wennberg, P. O., Hints, E. J. and Hanisco, T. F.:
20 OH in the tropical upper troposphere and its relationships to solar radiation and
21 reactive nitrogen, *J. Atmos. Chem.*, 71, 55-64, doi:10.1007/s10874-014-9280-2, 2014.
- 22 Garny, H., Grewe, V., Dameris, M., Bodeker, G. E. and Stenke, A.: Attribution of ozone
23 changes to dynamical and chemical processes in CCMs and CTMs, *Geosci. Model*
24 *Dev.*, 4, 271-286, doi:10.5194/gmd-4-271-2011, 2011.
- 25 Grewe, V., Dameris, M., Hein, R., Sausen, R. and Steil, B.: Future changes of the atmospheric
26 composition and the impact of climate change, *Tellus*, 53B, 103-121, 2001.
- 27 Grewe, V.: The origin of ozone, *Atmos. Chem. Phys.*, 6, 1495-1511, doi:10.5194/acp-6-1495-
28 2006, 2006.
- 29 Grewe, V.: Impact of Lightning on Air Chemistry and Climate, In: *Lightning: Principles,*
30 *Instruments and Applications Review of Modern Lightning Research*, Betz, Hans
31 Dieter; Schumann, Ulrich; Laroche, Pierre (Eds.), 524-551, Springer Verlag, 2009.

- 1 Guenther, A., Karl, T., Harley, P., Wiedinmyer, C., Palmer, P. I. and Geron, C.: Estimates of
2 global terrestrial isoprene emissions using MEGAN (Model of Emissions of Gases and
3 Aerosols from Nature), *Atmos. Chem. Phys.*, 6, 3181-3210, doi:10.5194/acp-6-3181-
4 2006, 2006.
- 5 Hegglin, M. I. and Shepherd, T. G.: Large climate-induced changes in ultraviolet index and
6 stratosphere-to-troposphere ozone flux, *Nat. Geosci.*, 2, 687-691,
7 doi:10.1038/ngeo604, 2009.
- 8 Ho, S., Edwards, D. P., Gille, J. C., Luo, M., Osterman, G. B., Kulawik, S. S. and Worden,
9 H.: A global comparison of carbon monoxide profiles and column amounts from
10 Tropospheric Emission Spectrometer (TES) and Measurements of Pollution in the
11 Troposphere (MOPITT), *J. Geophys. Res.*, 114, D21307, doi:10.1029/2009JD012242,
12 2009.
- 13 Huijnen, V., Eskes, H. J., Poupkou, A., Elbern, H., Boersma, K. F., Foret, G., Sofiev, M.,
14 Valdebenito, A., Flemming, J., Stein, O., Gross, A., Robertson, L., D'Isidoro, M.,
15 Kioutsioukis, I., Friese, E., Amstrup, B., Bergstrom, R., Strunk, A., Vira, J., Zyryanov,
16 D., Maurizi, A., Melas, D., Peuch, V.-H. and Zerefos, C.: Comparison of OMI NO₂
17 tropospheric columns with an ensemble of global and European regional air quality
18 models, *Atmos. Chem. Phys.*, 10, 3273-3296, doi: 10.5194/acp-10-3273-2010, 2010.
- 19 Kawase, H., Nagashima, T., Sudo, K. and Nozawa, T.: Future changes in tropospheric ozone
20 under Representative Concentration Pathways (RCPs), *Geophys. Res. Lett.*, 38,
21 L05801, doi:10.1029/2010GL046402, 2011.
- 22 Kley, D., Crutzen, P. J., Smit, H. G. J., Vömel, H., Oltmans, S. J., Grassl, H. and Ramanathan,
23 V.: Observations of near-zero ozone concentrations over the convective Pacific:
24 Effects on air chemistry, *Science*, 274, 230-233, doi:10.1126/science.274.5285.230,
25 1996.
- 26 Lamarque, J.-F., Bond, T. C., Eyring, V., Granier, C., Heil, A., Klimont, Z., Lee, D., Liousse,
27 C., Mieville, A., Owen, B., Schultz, M. G., Shindell, D., Smith, S. J., Stehfest, E., Van
28 Aardenne, J., Cooper, O. R., Kainuma, M., Mahowald, N., McConnell, J. R., Naik, V.,
29 Riahi, K. and van Vuuren, D. P.: Historical (1850-2000) gridded anthropogenic and
30 biomass burning emissions of reactive gases and aerosols: methodology and

1 application, *Atmos. Chem. Phys.*, 10, 7017-7039, doi:10.5194/acp-10-7017-2010,
2 2010.

3 Lamarque, J.-F., Shindell, D. T., Josse, B., Young, P. J., Cionni, I., Eyring, V., Bergmann, D.,
4 Cameron-Smith, P., Collins, W. J., Doherty, R., Dalsoren, S., Faluvegi, G., Folberth,
5 G., Ghan, S. J., Horowitz, L. W., Lee, Y. H., MacKenzie, I. A., Nagashima, T., Naik,
6 V., Plummer, D., Righi, M., Rumbold, S. T., Schulz, M., Skeie, R. B., Stevenson, D.
7 S., Strode, S., Sudo, K., Szopa, S., Voulgarakis, A. and Zeng, G.: The Atmospheric
8 Chemistry and Climate Model Intercomparison Project (ACCMIP): overview and
9 description of models, simulations and climate diagnostics, *Geosci. Model Dev.*, 6,
10 179-206, doi:10.5194/gmd-6-179-2013, 2013.

11 Lang, C., Waugh, D. W., Olsen, M. A., Douglass, A. R., Liang, Q., Nielsen, J. E., Oman, L.
12 D., Pawson, S. and Stolarski, R. S.: The impact of greenhouse gases on past changes in
13 tropospheric ozone, *J. Geophys. Res.*, 117(D23), doi:10.1029/2012JD018293, 2012.

14 Lin, M., Horowitz, L. W., Oltmans, S. J., Fiore, A. M. and Fan, S.: Tropospheric ozone trends
15 at Mauna Loa Observatory tied to decadal climate variability, *Nat. Geosci.*, 7, 136-
16 143, doi: 10.1038/NGEO2066, 2014.

17 Lin, S. J. and Rood, R. B.: Multidimensional flux-form semi-Lagrangian transport schemes,
18 *Mon. Weather Rev.* 124(9), 2046-2070, doi:http://dx.doi.org/10.1175/1520-
19 0493(1996)124<2046:MFFSLT>2.0.CO;2, 1996.

20 Masui, T., Matsumoto, K., Hijioka, Y., Kinoshita, T., Nozawa, T., Ishiwatari, S., Kato, E.,
21 Shukla, P. R., Yamagata, Y. and Kainuma, M.: An emission pathway for stabilization
22 at 6 Wm⁻² radiative forcing, *Climatic Change*, 109(1-2), 59-76, doi:10.1007/s10584-
23 011-0150-5, 2011.

24 Meehl, G. A., Washington, W. M., Arblaster, J. M., Hu, A., Teng, H., Kay, J. E., Gettelman,
25 A., Lawrence, D. M., Sanderson, B. M. and Strand, W. G.: Climate change projections
26 in CESM1(CAM5) compared to CCSM4, *J. Climate*, 26, 6287-6308,
27 doi:http://dx.doi.org/10.1175/JCLI-D-12-00572.1, 2013.

28 Morgenstern, O., Zeng, G., Abraham, N. L., Telford, P. J., Braesicke, P., Pyle, J. A.,
29 Hardiman, S. C., O'Connor, F. M. and Johnson, C. E.: Impacts of climate change,
30 ozone recovery, and increasing methane on surface ozone and the tropospheric

1 oxidizing capacity, *J. Geophys. Res.*, 118, 1028-1041, doi:10.1029/2012JD018382,
2 2013.

3 Murray, L. T., Jacob, D. J., Logan, J. A., Hudman, R. C. and Koshak, W. J.: Optimized
4 regional and interannual variability of lightning in a global chemical transport model
5 constrained by LIS/OTD satellite data, *J. Geophys. Res.*, 117, D20307,
6 doi:10.1029/2012jd017934, 2012.

7 Myhre, G., Shindell, D., Bréon, F.-M., Collins, W., Fuglestedt, J., Huang, J., Koch, D.,
8 Lamarque, J.-F., Lee, D., Mendoza, B., Nakajima, T., Robock, A., Stephens, G.,
9 Takemura, T. and Zhang, H.: Anthropogenic and natural radiative forcing, Chapter 8
10 in *Climate Change 2013: The Physical Science Basis. Contribution of Working Group*
11 *I to the Fifth Assessment Report of the Intergovernmental Panel on Climate Change*,
12 edited by Stocker, T. F., Qin, D., Plattner, G.-K., Tignor, M., Allen, S. K., Boschung,
13 J., Nauels, A., Xia, Y., Bex, V. and Midgley, P. M., Cambridge University Press,
14 Cambridge, United Kingdom and New York, NY, USA, 2013.

15 Naik, V., Voulgarakis, A., Fiore, A. M., Horowitz, L. W., Lamarque, J.-F., Lin, M., Prather,
16 M. J., Young, P. J., Bergmann, D., Cameron-Smith, P. J., Cionni, I., Collins, W. J.,
17 Dalsøren, S. B., Doherty, R., Eyring, V., Faluvegi, G., Folberth, G. A., Josse, B., Lee,
18 Y. H., MacKenzie, I. A., Nagashima, T., van Noije, T. P. C., Plummer, D. A., Righi,
19 M., Rumbold, S. T., Skeie, R., Shindell, D. T., Stevenson, D. S., Strode, S., Sudo, K.
20 Szopa, S. and Zeng, G.: Preindustrial to present-day changes in tropospheric hydroxyl
21 radical and methane lifetime from the Atmospheric Chemistry and Climate Model
22 Intercomparison Project (ACCMIP), *Atmos. Chem. Phys.*, 13, 5277-5298,
23 doi:10.5194/acp-13-5277-2013, 2013.

24 Parrish, D. D., Lamarque, J.-F., Naik, V., Horowitz, L. Shindell, D. T., Staehelin, J., Derwent,
25 R., Cooper, O. R., Tanimoto, H., Volz-Thomas, A., Gilge, S., Scheel, H.-E.,
26 Steinbacher, M. and Fröhlich, M.: Long-term changes in lower tropospheric baseline
27 ozone concentrations: Comparing chemistry-climate models and observations at
28 northern midlatitudes, *J. Geophys. Res.*, 119, 5719-5736, doi:10.1002/2013JD021435,
29 2014.

30 Poeschl, U., von Kuhlmann, R., Poisson, N. and Crutzen, P. J.: Development and
31 intercomparison of condensed isoprene oxidation mechanisms for global atmospheric
32 modeling, *J. Atmos. Chem.*, 37, 29-52, doi:10.1023/A:1006391009798, 2000.

- 1 Price, C. and Rind, D.: A simple lightning parameterization for calculating global lightning
2 distributions, *J. Geophys. Res.*, 97, 9919-9933, doi:10.1029/92JD00719, 1992.
- 3 Price, C. G.: Lightning Applications in Weather and Climate Research, *Surv. Geophys.*, 34,
4 755-767, doi:10.1007/s10712-012-9218-7, 2013.
- 5 Rayner, N. A., Parker, D. E., Horton, E. B., Folland, C. K., Alexander, L. V., Rowell, D. P.,
6 Kent, E. C. and Kaplan, A.: Global analyses of sea surface temperature, sea ice, and
7 night marine air temperature since the late nineteenth century, *J. Geophys. Res.*, 108,
8 4407, doi:10.1029/2002JD002670, 2003.
- 9 Revell, L. E., Bodeker, G. E., Smale, D., Lehmann, R., Huck, P. E., Williamson, B. E.,
10 Rozanov, E. and Struthers, H.: The effectiveness of N₂O in depleting stratospheric
11 ozone, *Geophys. Res. Lett.*, 39, L15806, doi:10.1029/2012GL052143, 2012.
- 12 Rex, M., Wohltmann, I., Ridder, T., Lehmann, R., Rosenlof, K., Wennberg, P., Weisenstein,
13 D., Notholt, J., Krüger, K., Mohr, V. and Tegtmeier, S.: A tropical West Pacific OH
14 minimum and implications for stratospheric composition, *Atmos. Chem., Phys.*, 14,
15 4287-4841, doi:10.5194/acp-14-4827-2014, 2014.
- 16 Richards, N. A. D., Osterman, G. B., Browell, E. V., Hair, J. W., Avery, M. and Li, Q.:
17 Validation of Tropospheric Emission Spectrometer ozone profiles with aircraft
18 observations during the Intercontinental Chemical Transport Experiment–B, *J.*
19 *Geophys. Res.*, 113, D16S29, doi:10.1029/2007JD008815, 2008.
- 20 Roeckner, E., Bäuml, G., Bonaventura, L., Brokopf, R., Esch, M., Giorgetta, M., Hagemann,
21 S., Kirchner, I., Kornblueh, L., Manzini, E., Rhodin, A., Schlese, U., Schulzweida, U.
22 and Tompkins, A.: The atmospheric general circulation model ECHAM 5. Part I:
23 Model description, Max-Planck-Institut für Meteorologie, Hamburg, Report No. 349,
24 http://www.mpimet.mpg.de/fileadmin/publikationen/Reports/max_scirep_349.pdf,
25 2003.
- 26 Rozanov, E., Schlesinger, M. E., Zubov, V., Yang, F. and Andronova, N. G.: The UIUC
27 three-dimensional stratospheric chemical transport model: Description and evaluation
28 of the simulated source gases and ozone, *J. Geophys. Res.*, 104, 11755-11781, 1999.
- 29 Schumann, U. and Huntrieser, H.: The global lightning-induced nitrogen oxides source,
30 *Atmos. Chem. Phys.*, 7, 3823-3907, doi:10.5194/acp-7-3823-2007, 2007.

- 1 Seinfeld, J. H. and Pandis, S. N.: Atmospheric Chemistry and Physics: From Air Pollution to
2 Climate Change, John Wiley and Sons, Inc., Hoboken, New Jersey, USA, 2nd edn.,
3 2006.
- 4 Shindell, D. T., Faluvegi, G., Koch, D. M., Schmidt, G. A., Unger, N. and Bauer, S. E.:
5 Improved attribution of climate forcing to emissions, *Science*, 326 (5953), 716-718,
6 doi:10.1126/science.1174760, 2009.
- 7 Silva, R. A., West, J. J., Zhang, Y., Anenberg, S. C., Lamarque, J.-F., Shindell, D. T., Collins,
8 W. J., Dalsoren, S., Faluvegi, G., Folberth, G., Horowitz, L. W., Nagashima, T., Naik,
9 V., Rumbold, S., Skeie, R., Sudo, K., Takemura, T., Bergmann, D., Cameron-Smith,
10 P., Cionni, I., Doherty, R. M., Eyring, V., Josse, B., MacKenzie, I. A., Plummer, D.,
11 Righi, M., Stevenson, D. S., Strode, S., Szopa, S. and Zeng, G.: Global premature
12 mortality due to anthropogenic outdoor air pollution and the contribution of past
13 climate change, *Environ. Res. Lett.*, 8, 034005, doi:10.1088/1748-9326/8/3/034005,
14 2013.
- 15 Singh, H. B., Gregory, G. L., Anderson, B., Browell, E., Sachse, G. W., Davis, D. D.,
16 Crawford, J., Bradshaw, J. D., Talbot, R., Blake, D. R., Thornton, D., Newell, R. and
17 Merrill, J.: Low ozone in the marine boundary layer of the tropical Pacific Ocean:
18 Photochemical loss, chlorine atoms, and entrainment, *J. Geophys. Res.*, 101(D1),
19 1907-1917, doi:10.1029/95JD01028, 1996.
- 20 Smyshlyaev, S. P., Mareev, E. A. and Galin, V. Ya.: Simulation of the impact of
21 thunderstorm activity on atmospheric gas composition, *Izv. Atmos. Ocean. Phys.*,
22 46(4), 451-467, 2010.
- 23 SPARC CCMVal: SPARC Report on the Evaluation of Chemistry-Climate Models, edited by:
24 Eyring, V., Shepherd, T. G., and Waugh, D. W., SPARC Report No. 5, WCRP-132,
25 WMO/TD-No. 1526, [http://www.sparc-climate.org/publications/sparc-reports/sparc-](http://www.sparc-climate.org/publications/sparc-reports/sparc-report-no5/)
26 [report-no5/](http://www.sparc-climate.org/publications/sparc-reports/sparc-report-no5/), 2010.
- 27 Stenke, A., Schraner, M., Rozanov, E., Egorova, T., Luo, B. and Peter, T.: The SOCOL
28 version 3.0 chemistry-climate model: description, evaluation, and implications from an
29 advanced transport algorithm, *Geosci. Model Dev.*, 6, 1407-1427, doi:10.5194/gmd-6-
30 1407-2013, 2013.

- 1 Stevenson, D. S., Young, P. J., Naik, V., Lamarque, J.-F., Shindell, D. T., Voulgarakis, A.,
2 Skeie, R. B., Dalsoren, S. B., Myhre, G., Berntsen, T. K., Folberth, G. A., Rumbold, S.
3 T., Collins, W. J., MacKenzie, I. A., Doherty, R. M., Zeng, G., van Noije, T. P. C.,
4 Strunk, A., Bergmann, D., Cameron-Smith, P., Plummer, D. A., Strode, S. A.,
5 Horowitz, L., Lee, Y. H., Szopa, S., Sudo, K., Nagashima, T., Josse, B., Cionni, I.,
6 Righi, M., Eyring, V., Conley, A., Bowman, K. W., Wild, O. and Archibald, A.:
7 Tropospheric ozone changes, radiative forcing and attribution to emissions in the
8 Atmospheric Chemistry and Climate Model Intercomparison Project (ACCMIP),
9 *Atmos. Chem. Phys.*, 13, 3063-3085, doi:10.5194/acp-13-3063-2013, 2013.
- 10 Thompson, A. M.: The oxidizing capacity of the Earth's atmosphere – probable past and
11 future changes, *Science*, 256, 1157–1165, doi:10.1126/science.256.5060.1157, 1992.
- 12 Toumi, R., Haigh, J. D. and Law, K. S.: A tropospheric ozone-lightning climate feedback.
13 *Geophys. Res. Lett.*, 23, 1037-1040, 1996.
- 14 Tsutsumi, Y., Makino, Y. and Jensen, J. B.: Vertical and latitudinal distributions of
15 tropospheric ozone over the western Pacific: Case studies from the PACE aircraft
16 missions, *J. Geophys. Res.*, 108(D8), doi:10.1029/2001JD001374, 2003.
- 17 Voulgarakis, A., Naik, V., Lamarque, J.-F., Shindell, D. T., Young, P. J., Prather, M. J., Wild,
18 O., Field, R. D., Bergmann, D., Cameron-Smith, P., Cionni, I., Collins, W. J.,
19 Dalsøren, S. B., Doherty, R. M., Eyring, V., Faluvegi, G., Folberth, G. A., Horowitz,
20 L. W., Josse, B., MacKenzie, I. A., Nagashima, T., Plummer, D. A., Righi, M.,
21 Rumbold, S. T., Stevenson, D. S., Strode, S. A., Sudo, K., Szopa, S. and Zeng, G.:
22 Analysis of present day and future OH and methane lifetime in the ACCMIP
23 simulations, *Atmos. Chem. Phys.*, 13, 2563-2587, doi:10.5194/acp-13-2563-2013,
24 2013.
- 25 Wang, C. and Prinn, G.: Impact of emissions, chemistry and climate on atmospheric carbon
26 monoxide: 100-year predictions from a global chemistry-climate model,
27 *Chemosphere*, 1, 73-81, 1999.
- 28 West, J. J., Szopa, S. and Hauglustaine, D. A.: Human mortality effects of future
29 concentrations of tropospheric ozone, *C. R. Geoscience*, 339, 775-783,
30 doi:http://dx.doi.org/10.1016/j.crte.2007.08.005, 2007.

1 Wild, O.: Modelling the global tropospheric ozone budget: exploring the variability in current
2 models, *Atmos. Chem. Phys.*, 7, 2643-2660, doi:10.5194/acp-7-2643-2007, 2007.

3 Wild, O., Fiore, A. M., Shindell, D. T., Doherty, R. M., Collins, W. J., Dentener, F. J.,
4 Schultz, M. G., Gong, S., MacKenzie, I. A., Zeng, G., Hess, P., Duncan, B. N.,
5 Bergmann, D. J., Szopa, S., Jonson, J. E., Keating, T. J. and Zuber, A.: Modelling
6 future changes in surface ozone: a parameterized approach, *Atmos. Chem. Phys.*, 12,
7 2037-2054, doi:10.5194/acp-12-2037-2012, 2012.

8 World Meteorological Organization: Scientific Assessment of Ozone Depletion: 2010, WMO
9 Global Ozone Research and Monitoring Project – Report No. 52, Geneva,
10 Switzerland, 2011.

11 Young, P. J., Archibald, A. T., Bowman, K. W., Lamarque, J. F., Naik, V., Stevenson, D. S.,
12 Tilmes, S., Voulgarakis, A., Wild, O., Bergmann, D., Cameron-Smith, P., Cionni, I.,
13 Collins, W. J., Dalsøren, S. B., Doherty, R. M., Eyring, V., Faluvegi, G., Horowitz, L.
14 W., Josse, B., Lee, Y. H., MacKenzie, I. A., Nagashima, T., Plummer, D. A., Righi,
15 M., Rumbold, S. T., Skeie, R. B., Shindell, D. T., Strode, S. A., Sudo, K., Szopa, S.,
16 and Zeng, G.: Pre-industrial to end 21st century projections of tropospheric ozone
17 from the Atmospheric Chemistry and Climate Model Intercomparison Project
18 (ACCMIP), *Atmos. Chem. Phys.*, 13, 2063-2090, doi:10.5194/acp-13-2063-2013,
19 2013.

20 Zeng, G., Morgenstern, O., Braesicke, P. and Pyle, J. A.: Impact of stratospheric ozone
21 recovery on tropospheric ozone and its budget, *Geophys. Res. Lett.*, 37, L09805,
22 doi:10.1029/2010GL042812, 2010.

23 Zhang, Y., Olsen, S. C., Dubey, M. K.: WRF/Chem simulated springtime impact of rising
24 Asian emissions on air quality over the U.S., *Atmos. Environ.*, 44, 2799-2812,
25 doi:10.1016/j.atmosenv.2010.05.003, 2010.

26 Zhang, H., Wu, S., Huang, Y. and Wang, Y.: Effects of stratospheric ozone recovery on
27 photochemistry and ozone air quality in the troposphere, *Atmos. Chem. Phys.*, 14,
28 4079-4086, doi:10.5194/acp-14-4079-2014, 2014.

29 Zubov, V., Rozanov, E. and Schleisinger, M. E.: Hybrid scheme for three-dimensional
30 advective transport, *Mon. Weather Rev.*, 127, 1335-1346, 1999.

31

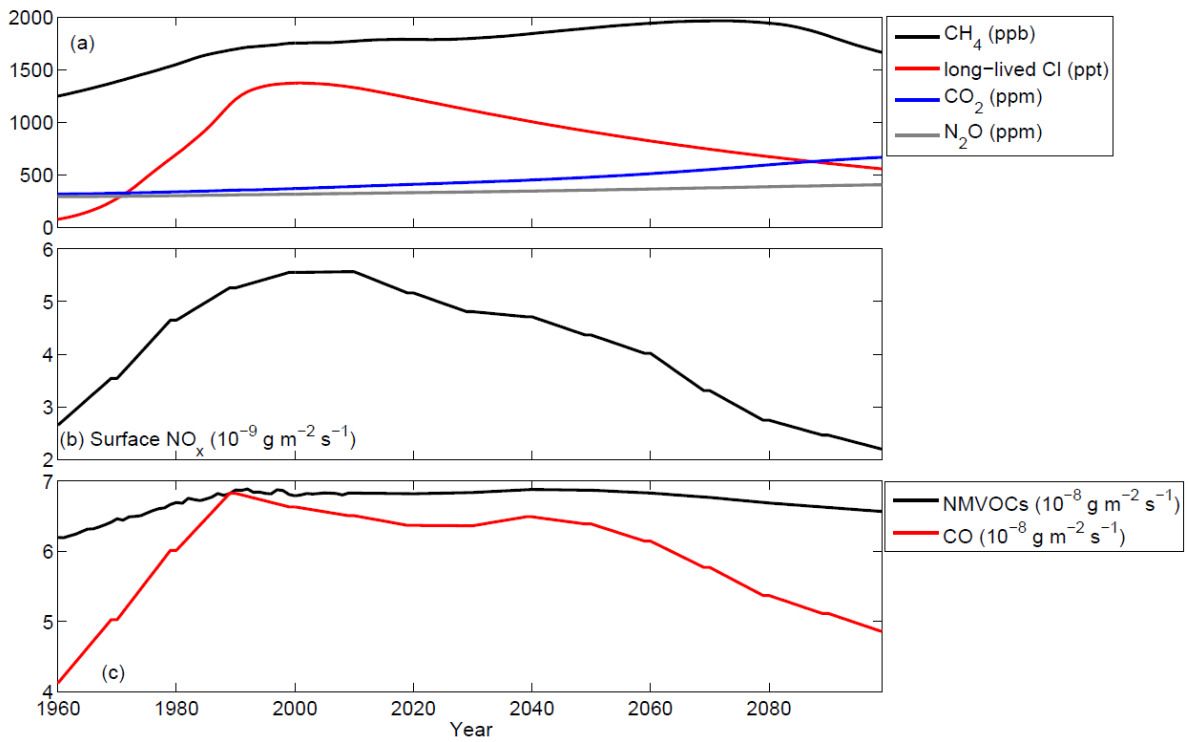
1 Table 1. Summary of boundary conditions used for the SOCOL CCM simulations

	REF-C2 (1960-2100)	fEmis (1960-2100)	fCH ₄ (1960-2100)
Greenhouse gases (CO ₂ , N ₂ O, CH ₄)	Observations until 2005 then RCP 6.0 (Masui et al., 2011).	Same as REF-C2.	CO ₂ and N ₂ O same as REF-C2; CH ₄ fixed at 1960 levels.
Ozone precursor emissions	Historical emissions until 2000 (Lamarque et al., 2010), then RCP 6.0.	Fixed at 1960 levels.	Fixed at 1960 levels.
SSTs	Observations until 2005 (Rayner et al., 2003), then RCP 6.0 (Meehl et al., 2013).	Same as REF-C2.	Same as REF-C2.
ODSs	The A1 scenario from WMO (2011), which includes observations until 2009.	Same as REF-C2.	Same as REF-C2.

2

3

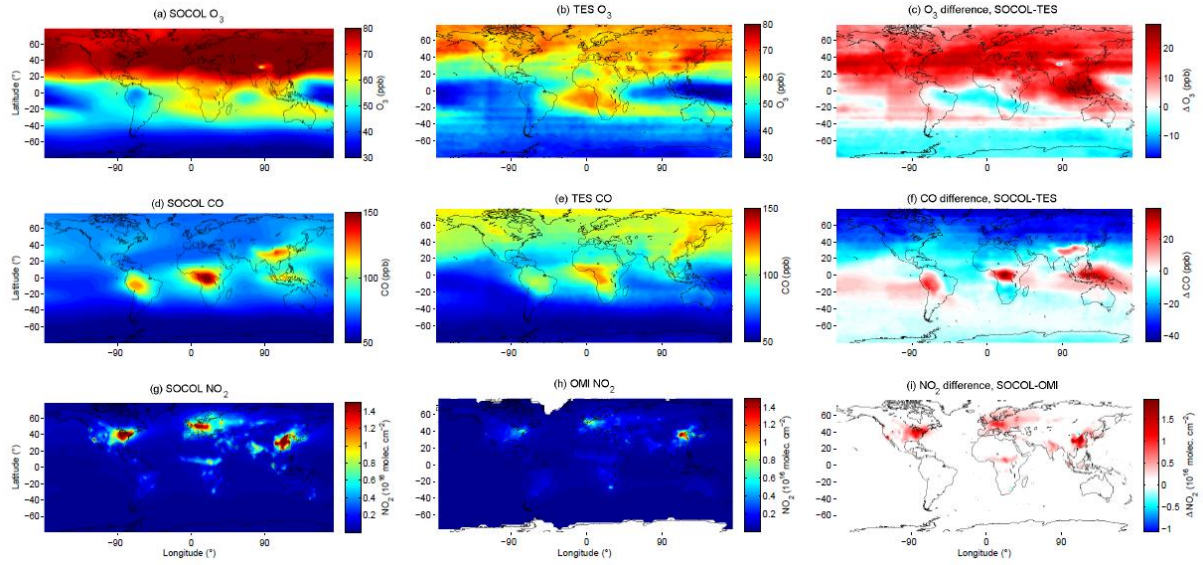
1
2



3
4
5
6
7
8
9

Figure 1. Boundary conditions used in the REF-C2 simulation (global-mean concentrations/emission fluxes). (a) CO₂, CH₄, N₂O mixing ratios following RCP 6.0, and long-lived chlorine mixing ratios following the WMO A1 scenario for ODSs. (b) Surface NO_x emission fluxes, following RCP 6.0. (c) Surface CO and NMVOC emission fluxes, following RCP 6.0.

1

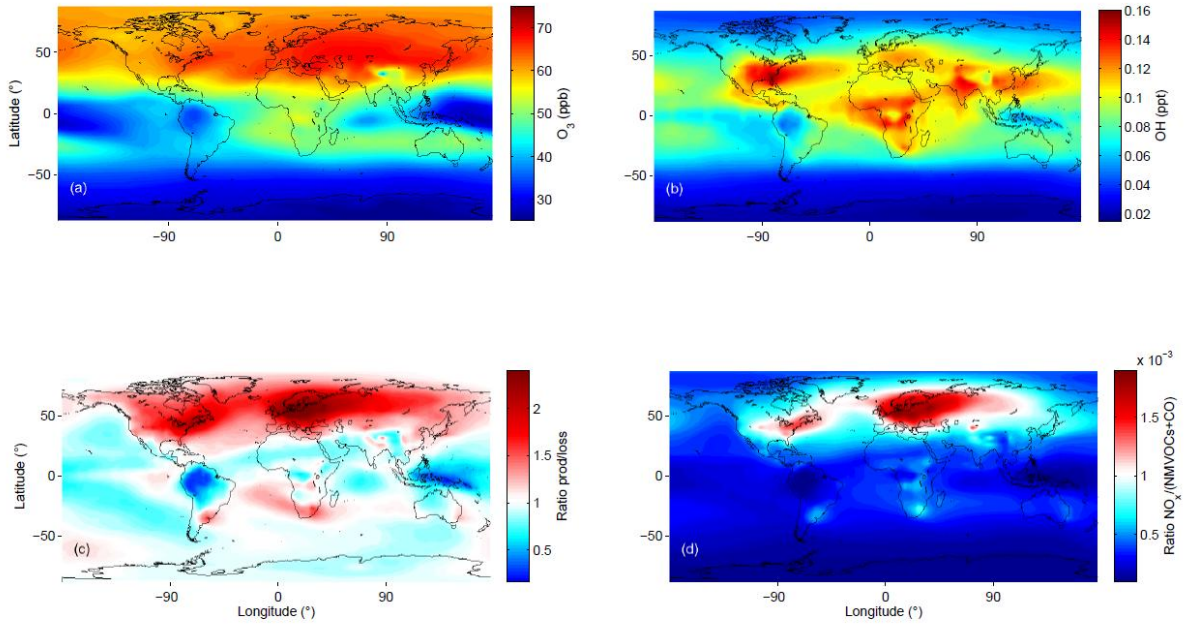


2

3

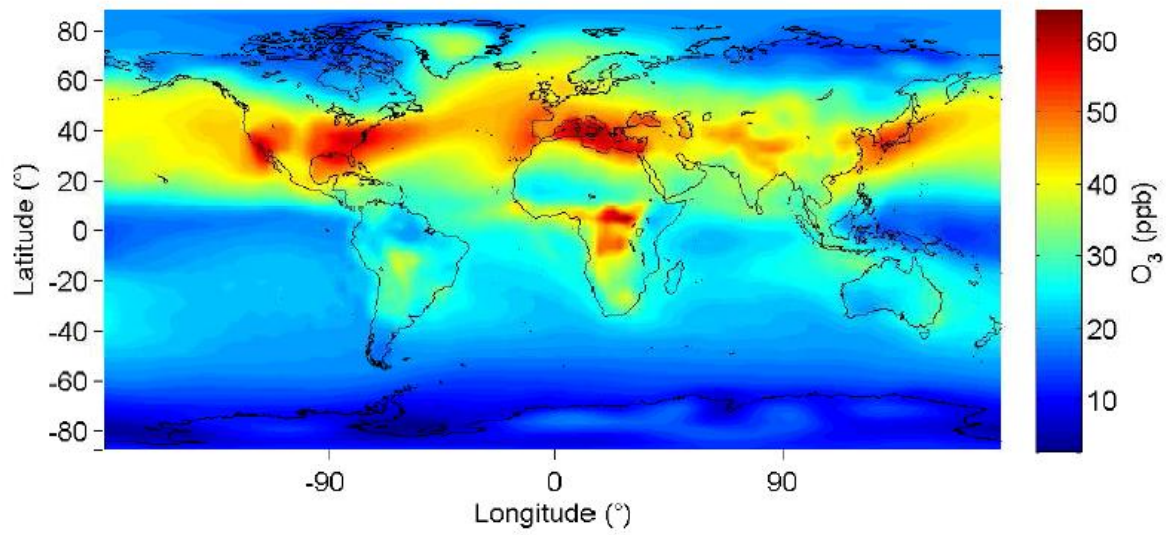
4 Figure 2. Comparisons of SOCOL model results (from the REF-C2 simulation) with
5 observations, averaged over 2005-2009, for: (a) SOCOL ozone, 500 hPa; (b) TES ozone, 464
6 hPa; (c) ozone difference (panel (a) minus (b)); (d) SOCOL CO, 500 hPa; (e) TES CO, 464
7 hPa; (f) CO difference (panel (d) minus (e)); (g) SOCOL tropospheric column NO_2 ; (h) OMI
8 tropospheric column NO_2 ; (i) NO_2 difference (panel (g) minus (h)).

9



1
2
3
4
5

Figure 3. Results from the REF-C2 simulation, 1960-1969 average, 500 hPa. (a) Ozone; (b) OH; (c) Ratio of ozone production over loss; (d) Ratio of NO_x : NMVOCs+CO.

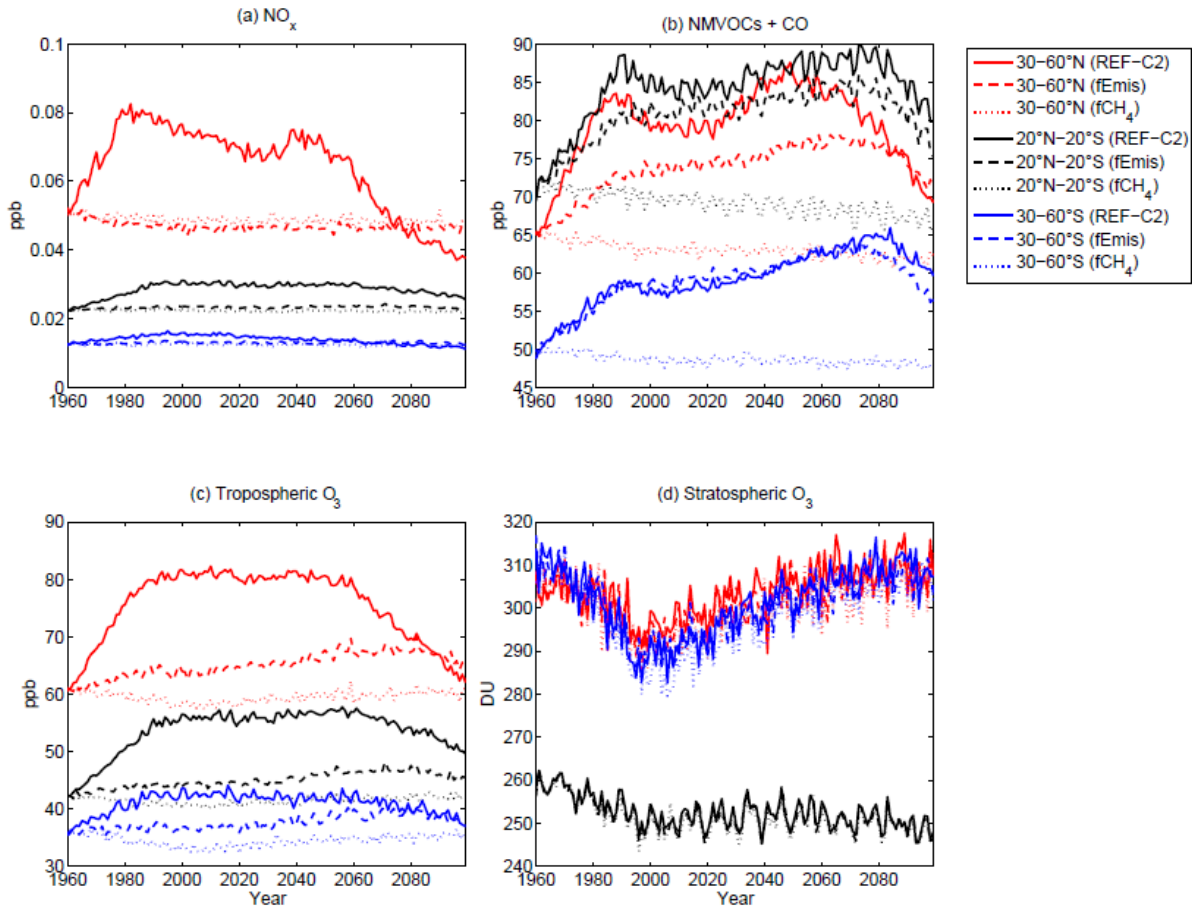


1

2 Figure 4. As for Figure 3a, but for the surface instead of 500 hPa.

3

1



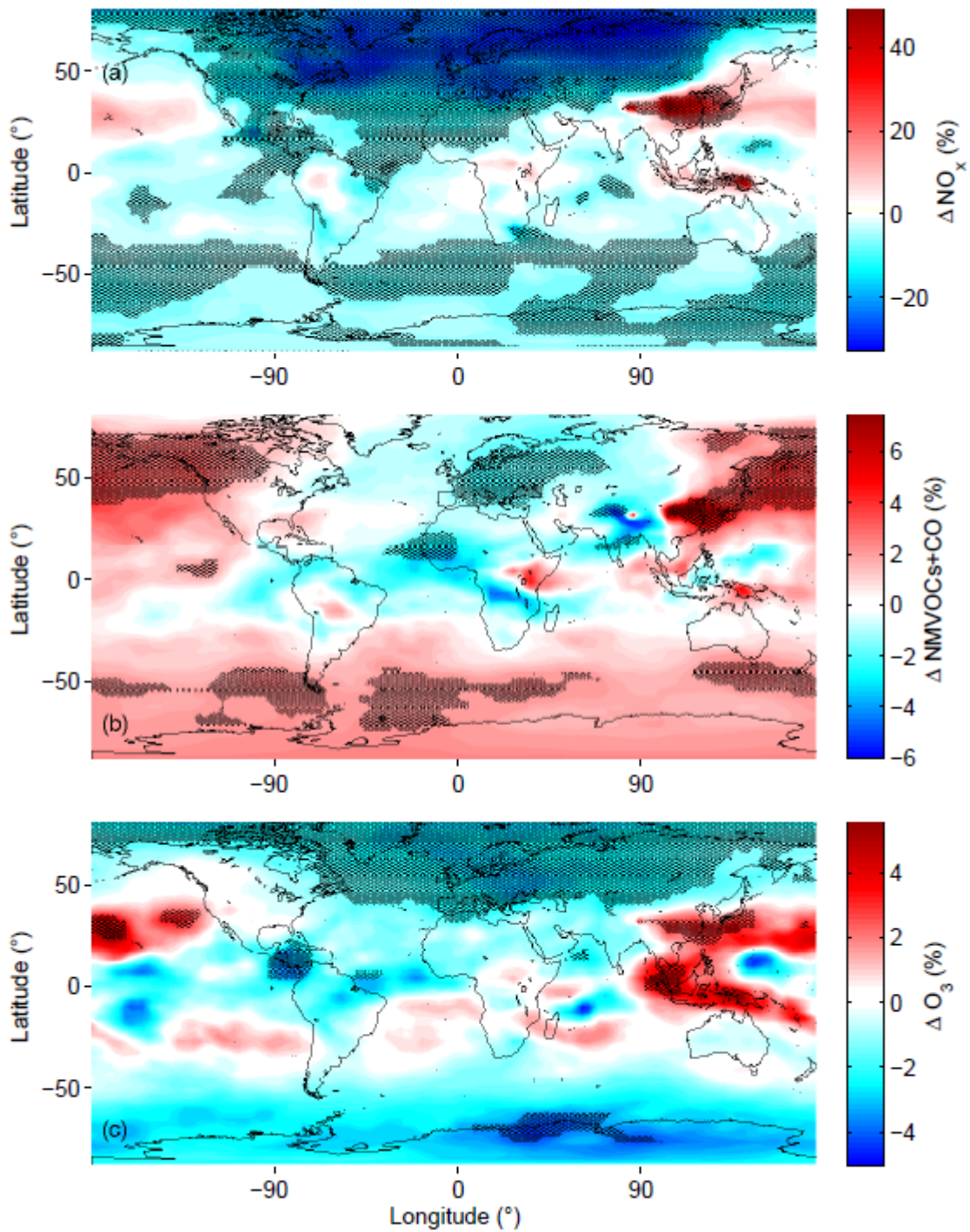
2

3

4 Figure 5. Timeseries of northern midlatitude (30-60°N, red lines), tropical (20°-20°S, black
5 lines) and southern midlatitude (30-60°S, blue lines): (a) NO_x (500 hPa); (b) NMVOCs + CO
6 (500 hPa); (c) tropospheric ozone (500 hPa); (d) stratospheric column ozone. Solid lines: for
7 the REF-C2 simulation. Dashed lines: fEmis simulation. Dotted lines: fCH₄ simulation.

8

1

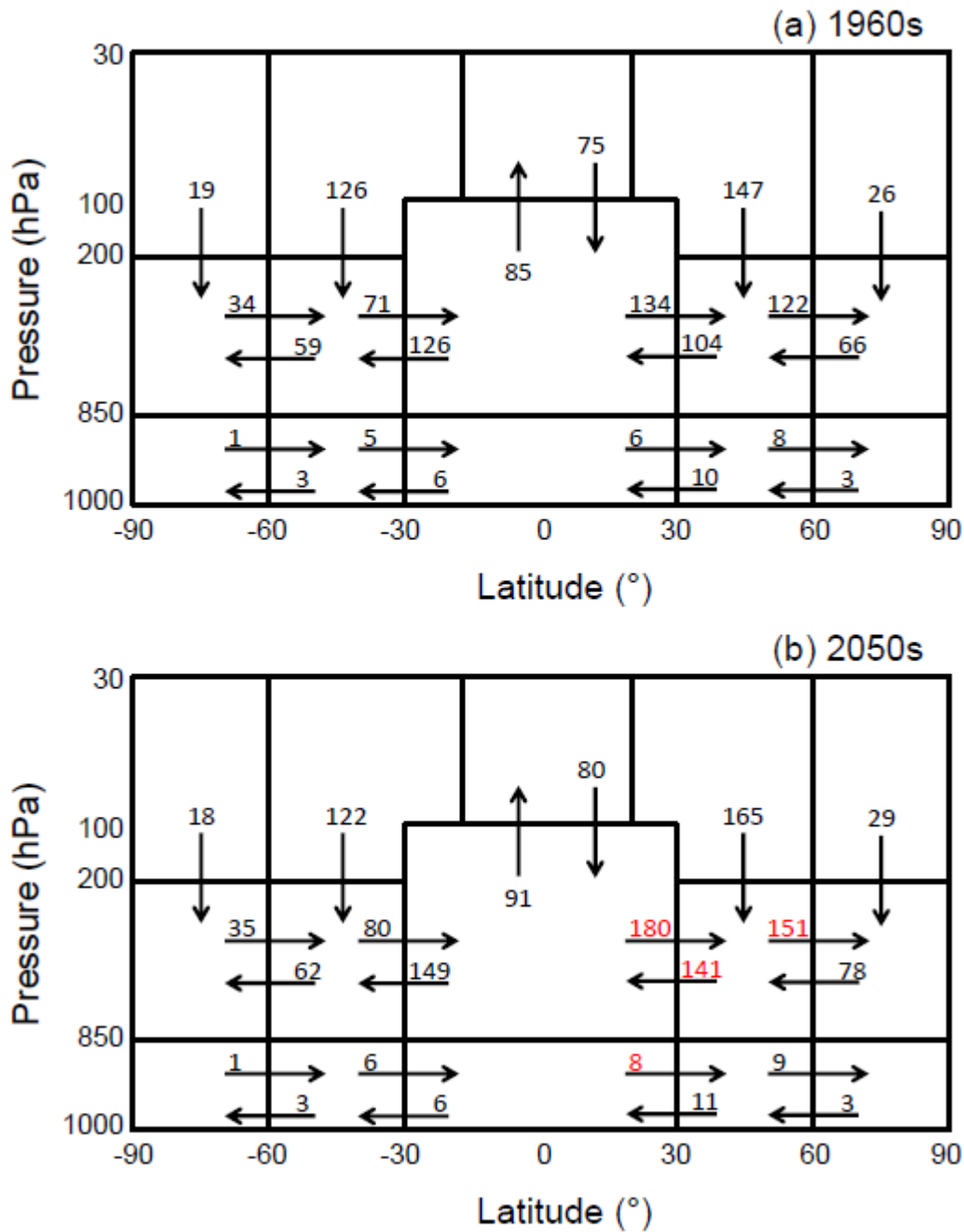


2

3 Figure 6. Changes between the 2000s and 2020s decades (2020s minus 2000s) in the REF-C2
4 simulation at 500 hPa for: (a) NO_x ; (b) NMVOCs+CO; (c) ozone. Shading indicates that the
5 difference is statistically significant at the 95% level of confidence.

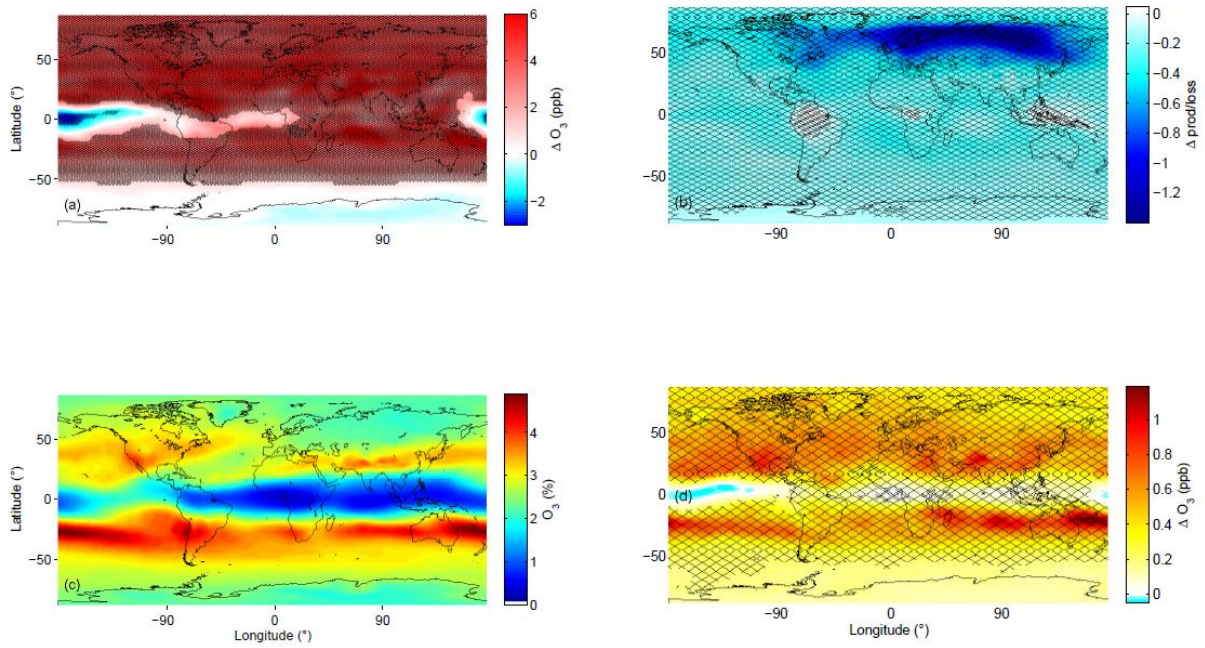
6

7



1
2
3
4
5
6
7

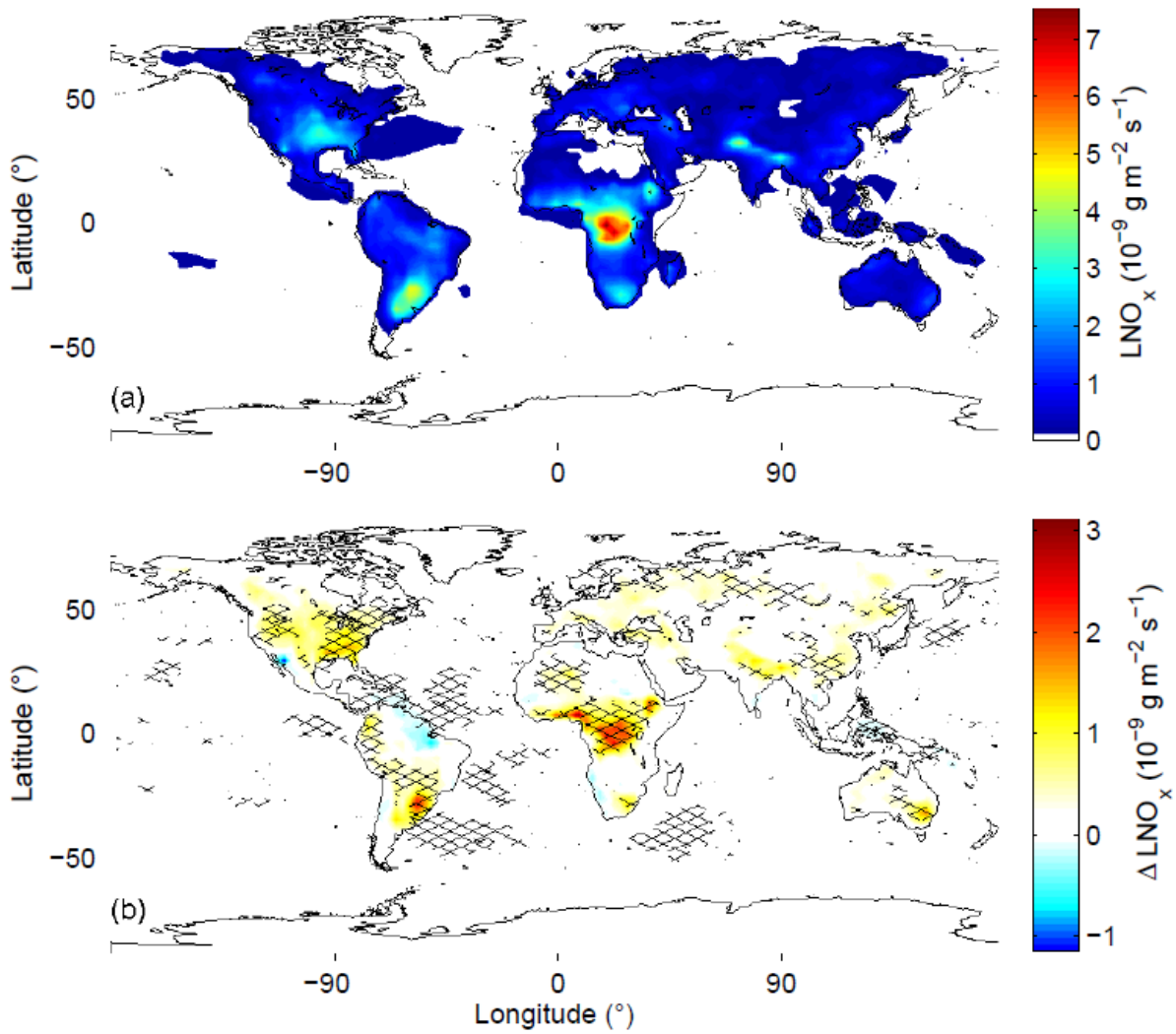
Figure 7. Decadal-mean ozone fluxes (Tg year⁻¹) between defined tracer regions for (a) the 1960s and (b) the 2050s in the REF-C2 simulation. Red text in panel (b) indicates an increase of more than 20% from the same quantity in (a).



1

2 Figure 8. (a) Change in ozone at 500 hPa in the fEemis simulation, 2090s minus 1960s; (b)
 3 Change in the ratio of ozone production over loss in the fEemis simulation, 2090s minus
 4 1960s; (c) Percentage of ozone at 500 hPa which was produced in the lower stratosphere in
 5 the fEemis simulation, 1960s decade; (d) Absolute change in the amount of ozone at 500 hPa
 6 which was produced in the lower stratosphere in the fEemis simulation, 2090s minus 1960s.
 7 Shading indicates that the difference is statistically significant at the 95% level of confidence.

8



1
 2 Figure 9. (a) Lightning NO_x emissions in the fEmis simulation, averaged over the 1960s; (b)
 3 Change in lightning NO_x emissions in the fEmis simulation, 2090s minus 1960s. Shading
 4 indicates that the difference is statistically significant at the 95% level of confidence.

5